# Widespread tungsten isotope anomalies and W mobility in crustal and mantle rocks of the Eoarchean Saglek Block, northern Labrador, Canada: Implications for early Earth processes and W recycling

Jingao Liu[1,*], Mathieu Touboul[2,**], Akira Ishikawa[3,4], Richard J. Walker[2], D. Graham Pearson[1]

[1] Department of Earth and Atmospheric Sciences, University of Alberta, 1-26 Earth Sciences Building, Edmonton, Alberta T6G 2E3 Canada
[2]Department of Geology, University of Maryland, College Park, Maryland, 20742 USA
[3]Department of Earth Science and Astronomy, University of Tokyo, 3-8-1 Komaba, Meguro, Tokyo 153-8902, Japan
[4]Research and Development Center for Submarine Resources, Japan Agency for Marine Earth Science and Technology (JAMSTEC), Yokosuka 236-0016, Japan

*Corresponding author: jingao@ualberta.ca

**Present address: Laboratoire de Géologie de Lyon, Ecole Normale Supérieure de, Lyon,

Labex LIO, Université Lyon 1, 46 Allée d'Italie 69364 Lyon Cedex 7, France.

Final Revisions to *Earth and Planetary Science Letters*

April 26, 2016 Version

## Abstract

Well-resolved $^{182}W$ isotope anomalies, relative to the present mantle, in Hadean-Archean terrestrial rocks have been interpreted to reflect the effects of variable late accretion and early mantle differentiation processes. To further explore these early Earth processes, we have carried out W concentration and isotopic measurements of Eoarchean ultramafic rocks, including lithospheric mantle rocks, meta-komatiites, a layered ultramafic body and associated crustal gneisses and amphibolites from the Uivak gneiss terrane of the Saglek Block, northern Labrador, Canada. These analyses are augmented by *in situ* W concentration measurements of individual phases in order to examine the major hosts of W in these rocks. Although the W budget in some rocks can be largely explained by a combination of their major phases, W in other rocks is hosted mainly in secondary grain-boundary assemblages, as well as in cryptic, unidentified W-bearing 'nugget' minerals. Whole rock W concentrations in the ultramafic rocks show unexpected enrichments relative, to elements with similar incompatibilities. By contrast, W concentrations are low in the Uivak gneisses. These data, along with the *in situ* W concentration data, suggest metamorphic transport/re-distribution of W from the regional felsic rocks, the Uivak gneiss precursors, to the spatially associated ultramafic rocks.

All but one sample from the lithologically varied Eoarchean Saglek suite is characterized by generally uniform ~ +11 ppm enrichments in $^{182}W$ relative to Earth's modern mantle. Modelling shows that the W isotopic enrichments in the ultramafic rocks were primarily inherited from the surrounding $^{182}W$-rich felsic precursor rocks, and that the W isotopic composition of the original ultramafic rocks cannot be determined. The observed W isotopic composition of mafic to ultramafic rocks in intimate contact with ancient crust should be viewed with caution in order to plate constraints on the early Hf-W isotopic evolution of the Earth's mantle with regard to late accretionary processes. Although $^{182}W$ anomalies can be erased via mixing in the convective mantle, recycling of $^{182}W$-rich crustal rocks into the mantle can produce new mantle sources with anomalous W isotopic compositions that can be tapped at much later times and, hence, this process should be considered as a mechanism for the generation of $^{182}W$-rich rocks at any subsequent time in Earth history.

**Keywords:** Tungsten, $^{182}W$ anomaly, recycling, peridotite, mantle, early Earth

## 1. Introduction

Deciphering the geochemical evolution of Earth's mantle is rooted in both spatial and temporal dimensions. The former primarily relies on seismic and magnetotelluric studies that reveal the physical and dynamic state of the present-day mantle at depth, while the latter is focused on the rock record through time. The destruction of crustal rocks by plate tectonics means that the rock record diminishes backward in time, hence, our view of the Earth in the Eoarchean and Hadean remains clouded. Nevertheless, new information about the early Earth is beginning to emerge from Hadean and younger materials as a result of the study of short-lived isotope systems. For example, $^{142}Nd/^{144}Nd$ ratio measurements show small variations among Archean rocks, compared with the modern mantle. These $^{142}Nd$ variations could only have been produced by mantle differentiation processes within the first ~500 Ma of Earth history, as a result of the decay of short-lived $^{146}Sm$ to $^{142}Nd$. The variations provide an important tool for tracing the formation and evolution of early-formed, diverse reservoirs (e.g., Boyet et al., 2003; Caro et al., 2003; Bennett et al., 2007; O'Neil et al., 2008; Rizo et al., 2011; Debaille et al., 2013; Roth et al., 2013).

In some recent W isotopic studies involving mafic/ultramafic rocks, it has been found that W abundances in such rocks are high and that there are broad similarities between the W isotopic compositions of crust and mantle rocks (e.g., Touboul et al., 2012, 2014; Rizo et al., 2016; Puchtel et al., 2016). Such observations raise questions concerning the mobility of W in the crust and the potential for post-crystallization W isotopic exchange between felsic and mafic/ultramafic rocks. In order to further explore the usefulness of the $^{182}Hf$-$^{182}W$ short-lived isotopic system in revealing early Earth processes when applied to mantle-derived mafic-ultramafic rocks, we examine Eoarchean ultramafic rocks, including lithospheric mantle rocks, meta-komatiites and a layered ultramafic body, from the Saglek Block of northern Labrador, Canada. We also examine associated tonalitic Uivak gneisses and amphibolite that surround the ultramafic rocks. Many of these rocks have been previously well characterized for their petrology, whole-rock major and trace element geochemistry, as well as Nd-Pb isotopes (Collerson et al., 1991; Wendt and Collerson, 1999). We report whole-rock W concentrations and W isotopic compositions for these rocks, as well as whole-rock major and trace element concentrations for Uivak gneisses and amphibolite. In addition, before applying W isotopic data to understand the geological processes responsible for the formation of these rocks, we evaluate the potential for W mobility and overprinting in these ancient rocks using *in situ* measurements of the abundances of W in constituent primary minerals and grain-boundary alteration assemblages, within a subset of these rocks. Whole-rock W abundance measurements are used along with modes calculated from mineral and bulk rock major element data to examine the mass balance for W.

## 2. Geological setting of the Saglek Block

The Saglek-Hebron area is located in northern Labrador, Canada, and is one of the oldest early Archean terranes, referred to as the Saglek Block. The block belongs to part of the North Atlantic Craton that ranges from NW Scotland through southern Greenland to Labrador (**Fig. 1**). It is divided by a major, NS-trending fault, termed the Handy fault, into two portions including a western region, characterized by granulite facies metamorphism, and an eastern region, characterized by sub-granulite to amphibolite facies metamorphism. The Saglek Block consists of Eo- to Neoarchean rock suites dominated by orthogneisses, but also includes metasedimentary

rocks, metavolcanics, ultramafic rocks and mafic-ultramafic dykes ("Saglek dykes" of Mesoarchean age), as well as younger ca. 2.5 Ga granites (Bridgwater et al., 1975; Collerson and Bridgwater, 1979; Schiøtte et al., 1989a,b; Komiya et al., 2015). On the basis of their geological relationships with the Saglek dykes, the orthogneisses in the Saglek Block can be classified into two groups (Bridgwater et al., 1975), analogous to the Ameralik dykes in the Itsaq Gneiss Complex, Greenland (McGregor, 1973). Orthogneisses older than the Saglek dykes are referred to as the Uivak Gneisses and include the Uivak I and II suites. Uivak I gneisses are characterized by tonalite-trondhjemite-granodiorite (TTG) compositions and are extensively distributed throughout the block, while the Uivak II gneisses are a suite of deformed feldspar granodioritic gneisses with simple fabrics, in marked contrast to the dominantly composite fabrics observed in the Uivak I gneisses. The boundaries between the Uivak I and II gneisses are often obscure, but from less strained outcrops, it can be seen that the Uivak I gneisses were intruded by Uivak II gneisses; the Uivak II gneiss has protoliths that were formed ca. 3.62 Ga (Schiøtte et al., 1989a,b). However, the age of the protoliths to the Uivak I gneisses is still under debate, ranging from 3.73 Ga (Schiøtte et al., 1989a,b), to >3.95 Ga (Komiya et al., 2015). In addition, the Lister gneiss is found as a post-Saglek dyke gneiss (ca. 3.24 Ga; Schiøtte et al., 1989a), and has been interpreted to have been tectonically juxtaposed against the early Archean "Uivak continent" (Schiøtte et al., 1990) or intruded into the Uivak gneisses (Collerson et al., 1976).

Based on the cross-cutting relationship with the Saglek dykes, the supracrustal rocks in the Saglek Block can also be divided into two groups, which are the pre-Saglek "Nulliak" group and the post-Saglek "Upernavik" group, respectively (e.g., Bridgwater et al., 1975; Collerson et al., 1976). Both groups, by and large, contain mafic and ultramafic rocks as well as rocks identified as chemical and clastic sedimentary rocks. The boundaries between the Nulliak supracrustal rocks and Uivak gneisses are often ambiguous in most places, but it is thought that the Uivak gneisses intruded the Nulliak supracrustal rocks in some places, while the Upernavik supracrustal rocks are younger than the Saglek dykes, but older than the ca. 3.24 Ga Lister gneiss. The exact ages of the Nulliak supracrustal rocks remain ambiguous (e.g., ca. 3.78 Ga, Schiøtte et al., 1989b; ca. 3.85 Ga, Nutman and Collerson, 1991; ca. 4.02 ± 0.19 Ga, Collerson et al., 1991), but they are considered to be older than the Uivak I gneisses (>3.73 Ga). Most recently, Komiya et al. (2015) interpreted the Nulliak supracrustal belt to be the oldest (>3.95 Ga) suite of supracrustal rocks, if the Uivak I gneiss is 3.95 Ga or older, and they concluded that the Nulliak supracrustal belt is part of an accretionary complex formed by some form of early plate tectonics. Conservatively, in this study, the Nulliak supracrustal rocks are assumed to be >3.8 Ga in age. In the Saglek Block, gneisses, supracrustal rocks and the Saglek dykes all underwent late Archean amphibolite to granulite facies reworking (e.g., Collerson and Bridgwater, 1979), most likely associated with the amalgamation of the North Atlantic Craton.

## 3. Samples

In this study, we investigate representative rocks from the Uivak I gneisses, amphibolite and the Nulliak supracrustal belt, across the Saglek Block (**Fig. 1**). Brief descriptions of these rocks are provided below.

*3.1. Uivak I gneiss*

In the Uivak I gneiss suite, three samples (KC91-17, SB-13 and SB-18) were analyzed for whole-rock major and trace element concentrations, including W, as well as bulk W isotopic compositions for KC91-17 and SB-13 and *in situ* elemental determination for SB-13. Sample KC91-17 is a tonalitic gneiss collected from the eastern coast of St. John's Harbour (**Fig. 1**). Sample SB-13 is a tonalitic gneiss consisting of 41% plagioclase, 41% quartz, 14% potassium feldspar and 4% biotite, while another tonalitic sample, SB-18, consists of 57% plagioclase, 28% quartz, 8% potassium feldspar and 8% biotite. Sample SB-13 was collected from Ukkalek Island, and SB-18 was collected from Shudham Island (**Fig. 1**).

*3.2. Amphibolite*

Sample SB-19 is an amphibolite collected from Shudham Island. The amphibolite unit is enclosed by Uivak I gneiss. The amphibolite consists of 70% pargasite, 28% plagioclase and 2% clinopyroxene. This sample was analyzed for mineral and whole-rock major and trace element compositions, as well as bulk W content and isotopic composition.

*3.3. Meta-komatiite suite from the Nulliak supracrustal belt*

One of the ultramafic rock suites from the Nulliak supracrustal belt studied is dominantly composed of olivine-pyroxene hornblendites, and believed to represent a sequence of meta-komatiites that underwent amphibolite facies metamorphism (Collerson et al., 1991), as evidenced by prominent amphibole reaction zones in contact with ambient gneisses in the field. This meta-komatiite suite has been previously well characterized for petrography, whole-rock major and trace element geochemistry, as well as Nd-Pb isotopes (Collerson et al., 1991; Wendt and Collerson, 1999). Five of these rocks were first analyzed for W contents, and three meta-komatiites (KC87-111E, KC87-111G, and KC87-111K) were then chosen for W isotopic analyses.

*3.4. Lithospheric mantle suite from the Nulliak supracrustal belt*

In addition to the meta-komatiite suite mentioned above, another ultramafic rock suite containing meta-peridotites and meta-pyroxenites/hornblendites was discovered within the Nulliak supracrustal belt (Collerson et al., 1991 and reference therein). This ultramafic rock suite is thought to be direct samples of early Archean residual lithospheric mantle, in light of its structural setting, lithological association, and mineral reactions. In the lithospheric mantle suite, fourteen samples (KC87-104 D, E; KC87-114 G,I,K; KC87-119A; KC87-102; KC87-106A; KC91-21 A, B; KC91-52 A-D), previously characterized for petrography, whole-rock major and trace element geochemistry, as well as Nd-Pb isotopes (Collerson et al., 1991; Wendt and Collerson, 1999) were analyzed for W concentrations. Eight were selected for W isotopic composition analyses.

The KC87 series samples were collected in the vicinity of Iterungnek Fjord and Jerusalem Harbour (**Fig. 1**), the KC91-52 series was collected from Big Island, and KC91-21 was collected from the eastern coast of St. John's Harbour. These rocks have experienced serpentinization and/or

subsequent amphibolite facies metamorphism, as indicated by occurrences of serpentine, amphibole and metamorphic olivine, as well as the scarcity of pyroxene. Two samples (KC87-104D and KC87-114K) were measured for *in situ* mineral major and trace element compositions.

### *3.5.Cape Uivak layered body from the Nulliak supracrustal belt*

The ultramafic layered body from the Cape Uivak locale contains harzburgites, wehrlites and pyroxenites that have undergone serpentinization and amphibolite facies metamorphism. In this rock suite, five harzburgites, two olivine hornblendites and two hornblendites were previously analyzed for mineral compositions, whole rock major and trace elements. These rocks were analyzed for W concentrations, and two samples (KC91-32A, E) were analyzed for W isotopic compositions. Sample KC91-32A was chosen for *in situ* analysis.

## 4. Analytical methods

Mineral major element compositions were determined on polished thick sections using a JEOL 8900 Electron Probe Micro-analyzer. Tungsten concentration data for minerals were obtained using *in situ* laser ablation together with inductively coupled plasma-mass spectrometry (ICP-MS). In addition, an attempt was made to measure W concentrations in multi-phase assemblages that represent grain-boundary alteration in some of the rocks, in order to look for evidence of W mobility during alteration or metasomatism. Such data cannot be assigned to a specific phase, and the ablation characteristics of multi-phase aggregates are likely to differ from the NIST glass. As such, it is difficult to quantify the uncertainties associated with those specific data. Nonetheless, the data are sufficient to demonstrate that for some rocks, significant W is hosted in the grain-boundary assemblages. Tungsten concentration data for secondary standards (e.g., NIST614) agree with the reference values within ±5%, and have external reproducibility of 6% at the 2σ level. For the sample phases, the uncertainties of W data negatively correlate with the W concentrations ranging from ~4% for phases with W >0.4 ppm to higher values for phases with lower concentrations, typically less than 30%, but as high as 100% for phases like olivine and plagioclase with ppb to sub-ppb W concentrations.

Sample powders were made from coarse grains/small chips using a motorized agate ball mill. Whole-rock major element compositions, as well as loss-on-ignition values, were determined by X-ray fluorescence on fused glass disks made from rock powders. Whole-rock trace element analyses were conducted via solution by ICP-MS at the University of Alberta using a *ThermoElement XR*. Whole-rock W concentrations were measured using isotope dilution via ICP-MS. High-precision W isotopic ratios were determined as $WO_3^-$ on a *Thermo Scientific Triton Plus* TIMS in a negative mode at the University of Alberta. Detailed chemical and analytical procedures are provided in the Electronic Supplement.

## 5. Results

The *in situ* W concentration data are reported in **Table 1**. Whole-rock tungsten concentration and isotopic data are provided in **Table 2**. Mineral major element data and whole-rock major and trace element compositions are provided in the Electronic Supplement (Table S1 & S2). Whole-rock major and lithophile trace element data are generally consistent within uncertainties with those previously reported in Collerson et al. (1991), where available.

*5.1. Whole-rock major and lithophile trace element compositions*

The major element compositions of Uivak gneisses, amphibolite and ultramafic rocks are consistent with their petrological character, as illustrated by the correlations between MgO and $Al_2O_3$ or Ni (**Fig. S1 A & B**). Heavy rare earth element (REE) concentrations are also correlated with major element indicators of melt depletion (e.g., MgO vs Yb; **Fig. S1 C**). The Uivak gneisses and amphibolite exhibit significantly higher concentrations of highly incompatible elements, such as large-ion lithophile elements, high field strength elements (HFSE), and light to middle REE, compared with the ultramafic rocks (**Fig. S2**).

*5.2. In situ W concentrations*

The W concentrations of minerals and grain-boundary assemblages in selected crustal and mantle rocks are plotted in **Fig. 2**. The W concentration characteristics of each sample are briefly described below.

*Uivak gneiss*: Sample SB-13 has four major phases (plagioclase, quartz, K-feldspar and biotite). Biotite has a high concentration of W (~2.0 ppm) compared to other phases (<0.1 ppm). The grain boundary assemblages can have variable W concentrations ranging from 0.08 to 1.3 ppm.

*Amphibolite*: Sample SB-19 contains three major phases (hornblende, plagioclase and clinopyroxene). Both hornblende and clinopyroxene have comparable W concentrations (0.5-0.7 ppm) that are significantly higher than coexisting plagioclase (<0.01 ppm).

*Dunite*: Sample KC87-104D contains three major phases (serpentine, chromite and magnetite) together with trace sulfides. Serpentine and chromite, as well as grain boundary regions, uniformly have similar W concentrations (~0.2 ppm). By contrast, magnetite and some sulfides, for instance heazelwoodite, can have W concentrations as high as 0.5 ppm.

*Harzburgite*: Sample KC91-32A is formed of three major phases (olivine, amphibole and Cr-magnetite). Orthopyroxene, Cr-magnetite and amphibole have comparable but low concentrations of W (0.06-0.08 ppm), while olivine has virtually no W. Grain boundary assemblages in the rock exhibit significant higher W concentrations (0.65-0.71 ppm).

*Meta-olivine websterite*: Sample KC87-114K contains three major phases (olivine, pargasite and spinel). Olivine and spinel both have very low concentrations of W (<0.02 ppm), while pargasite has a higher W concentration (0.13 ppm) that is, however, lower than the multi-phase grain boundary assemblage in this rock (0.3 ppm).

*5.3. Whole-rock tungsten abundances and isotopic compositions*

Among the ultramafic rocks from the Nulliak supracrustal belt, the meta-komatiite suite has relatively low W contents, ranging from 34 to 69 ppb, while the lithospheric mantle suite generally has significantly higher and more variable W contents, ranging from 53 to 697 ppb, with one sample containing 1.75 ppm. Ultramafic rocks from the Cape Uivak layered body display relatively homogeneous W abundances, ranging from 127 to 287 ppb, with an average of 200 ppb. The three tonalitic Uivak gneisses have relatively low W abundances, ranging from 64 to 132 ppb, while the amphibolite has a higher W content of 547 ppb. No prominent correlation exists between W and MgO, Ni or any other index of magmatic evolution/differentiation (**Fig. 3**).

All but one rock from the Saglek Block exhibit well resolved, positive $^{182}W$ anomalies (**Fig. 4**) relative to modern terrestrial samples studied to date (Willbold et al., 2011; Touboul et al., 2012; Rizo et al., 2016). The meta-komatiite suite has a mean $\mu^{182}W$ (where $\mu^{182}W$ is the deviation, in parts per million, of the $^{182}W/^{184}W$ ratio of a sample relative to the terrestrial reference standard) of +9.1 ± 3.4 (n=3; 2σ SD). The lithospheric mantle suite has $\mu^{182}W$ averaging +11.8 ± 7.0 (n=7; 2σ SD), excluding sample KC87-114G, which has no resolvable W isotopic anomaly ($\mu^{182}W$ = -2.6 ± 4.6; n=2; 2σ SD) from the terrestrial standard. The two Cape Uivak samples have a mean $\mu^{182}W$ of +9.4 ± 4.8 (n=2; 2σ SD). Collectively, the ultramafic rocks (including meta-komatiites, lithospheric mantle rocks and Cape Uivak layered body) with anomalous W isotopic compositions show no statistically meaningful difference in their average $\mu^{182}W$ at the ±4 ppm (2σ SD) level of reproducibility achieved in this study, and have an average $\mu^{182}W$ of +10.7 ± 5.9 (2σ SD).

The two tonalitic Uivak gneisses have similar $\mu^{182}W$ values (averaged at 11.0 ± 3.3; 2σ SD) that are also identical within uncertainty to that of the amphibolite ($\mu^{182}W$ = 10.4 ± 3.5; 2σ SD). These two tonalitic gneisses and the amphibolite give an average $\mu^{182}W$ of +10.8 ± 4.0 (n=3; 2σ SD), which is also identical, within uncertainty, to the W isotopic composition of the ultramafic rocks. Overall, all but one of the Saglek crustal and ultramafic rocks has a uniform $\mu^{182}W$ of +11 ± 3 (2σ SD).

## 6. Discussion

*6.1. Controls on the elemental budget of tungsten in crustal and mantle rocks of the Saglek Block*

One objective here is to determine which phases host W in the silicate rocks studied, and to evaluate the potential for W mobility during alteration and/or metasomatism and its possible consequences for W isotopes. For the 5 samples analyzed using *in situ* LA-ICP-MS (SB-13, SB-19, KC87-104D, KC91-32A, and KC87-114K), bulk-rock measurements of W can be compared with the "calculated" bulk W concentrations achieved by combining *in situ* mineral W concentrations with mineral modal abundance estimates calculated using the MINSQ program (Herrmann and Berry, 2002) from EPMA mineral and bulk rock XRF data (Table S1 & S2).

The *in situ* W concentration data indicate that different phases control the W budget in different rock types (**Fig. 2**). In samples SB-13 (tonalite), SB-19 (amphibolite) and KC87-104D (serpentinized dunite), the calculated bulk rock W concentration matches the measured one, which suggests that there are no significant W-bearing "nugget" minerals in these rocks. For sample SB-13, biotite is the major W-host phase accounting for ~62 % of the W in the rock, while the other phases (e.g., plagioclase, K-feldspar and quartz) and grain-boundary assemblages have minor W budgets. For sample SB-19, hornblende is the dominant phase hosting ~84 % of the W in the rock.

For sample KC87-104D, the W is controlled by serpentine that accounts for ~86 % of the W in the rock. The trace sulfides present (pentlandite and heazelwoodite) have W contents that are at the sub-ppm level (**Table 1**), and thus are not major sites for W, consistent with the low partition coefficients (<1) of W between sulfide liquid and silicate melt in the upper mantle conditions (Li and Audétat, 2012).

The calculated W concentrations for samples KC91-32A (harzburgite) and KC87-114K (websterite), in contrast to the rocks noted above, are much lower than the measured concentrations (**Table 1**; **Fig. 2**). The missing W is probably hosted in W-bearing nugget minerals and/or at grain boundaries that contain higher W concentrations than major minerals in these rocks (**Fig. 2**). For sample KC91-32A, all major phases (olivine, orthopyroxene, amphibole and magnetite) have W contents (<0.1 ppm) that are lower than the measured bulk concentration (0.28 ppm). By contrast, the grain-boundary alteration assemblages have significantly higher W concentrations (0.65-0.71 ppm), therefore dominating the bulk concentration, in addition to potential W-bearing nugget minerals. Similarly, for websterite sample KC87-114K, all major phases (olivine, pargasite, magnetite and spinel), as well as grain-boundary assemblages, have W contents (<0.4 ppm) much lower than the measured bulk concentration (1.75 ppm), requiring the occurrence of W-bearing nugget minerals in this rock.

Collectively, hydrous minerals and grain-boundary assemblages, such as biotite, amphibole and serpentine, as well as in cryptic, unidentified W-bearing nugget minerals, can house significant amounts (as high as ~90%) of the W in the examined crustal and mantle rocks. Formation or decomposition of these W-bearing phases during secondary processes could cause mobilization of the W in the rocks. This possibility is discussed below in the context of the complex W concentration and isotope systematics of the Saglek rocks.

### *6.2. Origin of tungsten in Eoarchean crustal and mantle rocks of the Saglek Block*

Tungsten is a moderately siderophile element that also has chalcophile tendencies. During igneous processes on Earth, W behaves as a highly incompatible element, to an extent that is similar to U, Ba or Th (e.g., Arevalo and McDonough, 2008; König et al., 2008). Although W occurs as a highly charged cation in nature, like the HFSE Zr, Hf, Nb and Ta, it is significantly more mobile due to its ability to form soluble anion complexes. In terrestrial weathering/alteration environments, W can be slightly more mobile than Th and U, but is typically less mobile than Ba (e.g., König et al., 2008). Thus, assessing whether or not W concentrations co-vary with any of these elements can potentially shed light on the origin of W in the Saglek rocks.

Saglek ultramafic rocks, including amphibolite, meta-komatiites, lithospheric mantle rocks, and those from the Cape Uivak layered body, show variable extents of W enrichment relative to U, Ba, Th, and HFSE (**Fig. 5**), confirming that in these rock systems, W was even more mobile than Ba. In general, the extent of W enrichment increases with increasing MgO (**Fig. 3**). The W enrichment in the peridotitic samples, for instance with W/Th ratios as high as 13.9, compared with an average ratio of ~0.17 in MORB (König et al., 2011), contrasts with its highly incompatible nature, and most likely indicates selective W enrichment, after extensive melt depletion, for example through serpentinization/amphibolite facies metamorphism discussed above. Such W enrichment accounts for W concentrations (typical >100 ppb) in these rocks (**Table 2**) that are

higher than should be if they were pristine upper mantle rocks. Although the meta-komatiite suite has generally lower W concentrations (34 to 69 ppb) that seem to be of magmatic origin, their W/Th (0.4 to 0.9) are higher than the MORB value. Thus, compared to the peridotitic suite, the meta-komatiite suite has similar W enrichment, but to a less extent, which is consistent with the occurrence of amphibolite facies metamorphism and formation of W-rich massive hornblende. By comparison, the Uivak felsic gneisses show prominent W depletions (**Fig. 5; Fig. S3**) that are complementary to the W enrichment observed in the associated ultramafic rocks. This spatial coincidence in the enrichment and depletion of W between the Uivak intrusive granitoid rocks and their adjacent ultramafic rocks is the reverse of the relationship expected from consideration of the compatibility of W during magmatic differentiation. The relative differences in W concentrations may indicate that regional granulite-amphibolite facies metamorphism led to the mobilization of W hosted in the Uivak granitoid rocks and its transport and incorporation into the adjacent ultramafic rocks.

### 6.3. *Quantifying W exchange in the crust between ultramafic and felsic rocks in the Saglek Block*

From the discussion above, the metasomatic/metamorphic addition of W to highly-depleted residual mantle rocks, such as the dunites and harzburgites of the Saglek lithospheric mantle suite, and even the meta-komatiite suite, could partially or completely obscure the original W isotopic signature in the precursor rocks. Here we try to determine the impact of metasomatic W addition to the W isotopic signature in the original unaltered precursors of ultramafic rocks. Typical metamorphism and/or secondary alteration experienced by ultramafic and felsic rocks means that the absolute abundances of elements with similar magmatic incompatibilities, for example W, U and Th, may have changed in step with the volume/density change. Because Th is a fluid-immobile element compared to more fluid-mobile U, and assumed to remain intact relative to W, we use the elemental W/Th ratio, instead of W/U ratio to estimate the level of W enrichment. The similar silicate melt – solid incompatibilities of W and Th are interpreted to mean that that magmatic processes will not significantly fractionate the W/Th ratio from that of the mantle source, a prediction in keeping with the similar W/Th values observed between the primitive mantle (0.19; McDonough and Sun, 1995), MORB (~0.17; König et al., 2011) and the upper or bulk continental crust (0.18; Rudnick and Gao, 2014).

The W enrichment for a rock is calculated by:

$$W_{enrichment} = \frac{(\frac{W}{Th})_{rock} - (\frac{W}{Th})_{PM}}{(\frac{W}{Th})_{rock}} \times 100\% \quad (1)$$

where $(\frac{W}{Th})_{rock}$ is the measured ratio of the rock, and $(\frac{W}{Th})_{PM}$ is the ratio of the primitive mantle (0.19).

The W isotopic composition of a rock after W enrichment is given by:

$$\mu^{182}W_{rock} = \mu^{182}W_{precursor} \times (1 - W_{enrichment}) + \mu^{182}W_{enrichment} \times W_{enrichment} \quad (2)$$

where $\mu^{182}W_{enrichment}$ is given by the $\mu^{182}W$ of the Uivak gneisses (+11.0; **Table 2**), and $\mu^{182}W_{precursor}$ of the original unaltered precursor of the ultramafic rock is defined individually after

two endmembers spanning the $\mu^{182}W$ range observed in terrestrial samples with Source 1 having $\mu^{182}W = 0$ (modern mantle) and Source 2 having $\mu^{182}W = +21$ (i.e., the upper limit of the terrestrial samples measured to date; Rizo et al., 2016). All the uncertainties for $\mu^{182}W$ values are assumed to be ±4 (i.e., ±4 ppm) that is the reproducibility achieved in typical multi-static N-TIMS measurements (Touboul and Walker, 2012). Calculated model results in $\mu^{182}W$ versus W/Th space are depicted in **Fig. 6**.

Based on the Equation (1), for the Saglek ultramafic rocks the W enrichment ranges from 50 to 78 % for the meta-komatiite suite, 75 to 98% for the lithospheric mantle suite, 95 to 97% for the Cape Uivak layered body, and 88% for the amphibolite. These apparent enrichments are mirrored by accompanying severe W depletion in the Uivak gneisses, which ranges from 80 to 98%. Within current analytical uncertainties, as shown in **Fig. 6** the W isotopic compositions of all the ultramafic rocks (except KC87-114G) can be essentially explained by greater than 50% of their W originating from the Uivak felsic precursors regardless of the W isotopic composition of the mantle source. Given the substantial enrichment of W in the ultramafic rocks (orders of magnitude greater than any modelled melt residue), we could not constrain the W isotopic composition of their precursor rocks. Thus, we view it as unsafe to place too much weight on the interpretation of the W isotopic compositions in any of the ultramafic rocks, even though some of them could, in theory, represent their mantle source compositions. Instead, the observed W isotopic compositions of the ultramafic rocks were clearly primarily inherited from the precursors of the Uivak felsic gneisses. This process of W mobility and exchange/overprinting is consistent with the generally uniform W isotopic compositions of the entire Saglek rock suite, with an average for the crustal and mantle rocks of $\mu^{182}W \sim +11 \pm 3$ (**Fig. 4**). For sample KC87-114G with $\mu^{182}W$ close to zero, the source of W enrichment could have come from the materials with W isotopic composition like modern mantle.

### 6.4. *Implications of W isotopic anomalies in a wide spectrum of Eoarchean rocks*

A compilation of W isotope data recently reported for terrestrial rocks is shown in **Fig. 7.** Well-resolved, positive W isotope anomalies appear to be common in ancient rocks (Willbold et al., 2011, 2015; Touboul et al., 2012, 2014; Rizo et al., 2016; Puchtel et al., 2016). The data presented in this study represent the first W isotopic data measured in residual mantle peridotites. Highly siderophile elements (HSE) are best used as a tool to evaluate the extent of late accretion to Earth and the Moon (Becker et at., 2006; Day et al., 2007; Walker, 2009; Fischer-Gödde et al., 2011, 2012; Day and Walker, 2015), and, thus, are applied to explain the W isotopic anomalies in the lunar and terrestrial mantle from the perspective of late accretionary processes (e.g., Touboul et al., 2012, 2014, 2015; Kruijer et al., 2015; Willbold et al., 2015). However, the overprinting of the W abundances and isotopic compositions documented in the Eoarchean mantle peridotites and other ultramafic rocks from the Saglek Block indicates that there is no genetic correlation between mobile W and less mobile HSE in these ultramafic rocks. Similar evidence for potential overprinting of W isotopic compositions in ancient rocks is observed in the Nuvvuagittuq and Isua supracrustal rocks (Touboul et al., 2014; Rizo et al., 2016). Therefore, the HSE abundances, at least in ultramafic rocks measured so far, cannot be used to constrain what their W isotopic compositions offer as information for constraining late accretionary processes during Earth's early

mantle evolution. In contrast, the widespread $^{182}$W-enrichments in the Saglek rock suite appear to be dominated by the host crustal rocks and their W isotopic compositions offer further constraint on Earth's early evolution. Of note, the Saglek crustal rock suite has average $^{182}$W enrichment of ~11 ppm, which is, however, resolvably lower than those of other ancient rock suites investigated to date (average $\mu^{182}W = +15$; **Fig. 7**). The cause for such difference in W isotope anomalies is unclear.

The Eoarchean age of the Uivak I gneisses (Schiøtte et al., 1989b; Collerson et al., 1991; Komiya et al., 2015) indicates that they formed at least 500 Ma after solar system formation, and this places bounds on the origin of their W isotopic anomalies. The Sr isotope systematics of the Uivak I gneisses indicate that they were derived from melting of mafic lower crustal precursors with short crustal residence times (Bridgwater and Collerson, 1976). Thus, the W isotopic anomalies in the Eoarchean Uivak felsic precursor rocks were derived from a $^{182}$W-enriched mantle source that survived subsequent mixing for at least 500 Ma. This mantle source either incorporated the $^{182}$W-enriched isotopic signature of a differentiation event in Earth's mantle that occurred within the first 50 Ma of solar system formation when $^{182}$Hf had been extant, or it received less addition of late accreted material compared to today's BSE. The study of $^{142}$Nd systematics of the Uivak gneisses may potentially shed light on the first scenario, while to prove the second scenario, an estimate of HSE abundances in the mantle source of the hypothetical mafic crust from which the Uivak precursor granitoids were derived is required. However, due to the poorly constrained partitioning behavior of HSE during granitoid formation and their multi-stage evolution it remains impossible to accurately constrain the HSE abundances within the mantle source of granitoid rocks.

Small magnitude $^{142}$Nd anomalies relative to the terrestrial standard appear in rocks younger than 3.5 Ga on Earth (Debaille et al., 2013; Rizo et al., 2013), indicating the attenuation of $^{142}$Nd anomalies in the mantle over time, probably as a result of mixing of early-differentiated mantle reservoirs within 1 Ga in Earth history. Likewise, many early-formed and potentially extreme W isotopic anomalies in Earth's mantle may have been largely erased via mixing in the convective mantle. However, unlike fluid-immobile Nd, the high secondary mobility of W shown here in the Eoarchean Saglek rock suite indicates that recycling of $^{182}$W-rich crustal rocks into the mantle could have produced new mantle sources with positive $\mu^{182}$W anomalies, much later in the Archean, to account for observations of positive $\mu^{182}$W anomalies in Neoarchean rocks such as the ca. 2.8 Ga Kostomuksha komatiites (**Fig. 7**). These much younger manifestations of isotopically anomalous W, coupled with the ease with which elevated crustal W concentrations can overwhelm the W isotopic composition of highly depleted mantle, suggest that $^{182}$W-rich signatures preserved in ancient crustal rocks could potentially prolong the existence of enriched $^{182}$W signatures in even younger mantle-derived rocks through subsequent subduction recycling and incomplete mantle mixing.

## 7. Conclusions

1) Eoarchean felsic, mafic and ultramafic rocks from the Saglek Block, northern Labrador have widely varying bulk W abundances that cannot be linked to primary petrogenetic processes.

2) The systematics of W behavior relative to lithophile elements in the Saglek rocks, combined with evidence from *in-situ* measurements of abundant grain-boundary W in the ultramafic rocks suggests significant secondary W mobility in amphibolite-granulite facies domains.
3) The complementary enrichment and depletion of W contents in ultramafic rocks and the surrounding Uivak gneisses suggests metamorphic remobilization of W from crustal granitoids into embedded ultramafic rocks.
4) All but one of the 16 measured Eoarchean Saglek rocks are characterized by similar $^{182}W$ enrichments of $+11 \pm 3$ ppm relative to the present mantle.
5) Modelling shows that the anomalous W isotopic signatures in the Saglek ultramafic rocks were primarily derived from the surrounding felsic precursor rocks, and thus, there is no genetic correlation between mobile W and less mobile HSE in such ultramafic rocks. As such, the HSE abundances at least in these ultramafic rocks cannot be used to constrain what their W isotopic compositions offer as information for constraining late accretionary processes during Earth's early mantle evolution.
6) The W isotopic anomalies in the Eoarchean Uivak felsic precursor rocks were derived from $^{182}W$-enriched mantle sources that survived subsequent mixing for at least 500 Ma.
7) Although $^{182}W$ anomalies can be erased via mixing in the convective mantle, recycling of $^{182}W$-rich crustal rocks into the mantle can produce new mantle sources with anomalous W isotopic compositions that can be tapped at much later times in Earth history. Crustal recycling of Eoarchean rocks with $^{182}W$ anomalies should be considered as a mechanism for the generation of $^{182}W$-rich rocks at any subsequent time in Earth history.

## Acknowledgements

This research was supported by funding from the NSERC Discovery Grants program to DGP and U.S. NSF-CSEDI grant EAR1265169 (to RJW). We thank Andrew Locock and Tom Chacko for providing assistance in the EMPA analyses, Yan Lou for help with the laser ablation measurements, and Sarah Woodland and Garrett Harris for help in the lab. Editor Bernard Marty and three anonymous reviewers are thanked for improving the focus of this manuscript.

## References


Arevalo, R., McDonough, W.F., 2008. Tungsten geochemistry and implications for understanding the Earth's interior. Earth and Planetary Science Letters 272, 656-665.

Becker, H., Horan, M.F., Walker, R.J., Gao, S., Lorand, J.P., Rudnick, R.L., 2006. Highly siderophile element composition of the Earth's primitive upper mantle: Constraints from new data on peridotite massifs and xenoliths. Geochimica et Cosmochimica Acta 70, 4528-4550.

Bennett, V.C., Brandon, A.D., Nutman, A.P., 2007. Coupled $^{142}$Nd-$^{143}$Nd isotopic evidence for Hadean mantle dynamics. Science 318, 1907-1910.

Boyet, M., Blichert-Toft, J., Rosing, M., Storey, M., Telouk, P., Albarede, F., 2003. $^{142}$Nd evidence for early Earth differentiation. Earth and Planetary Science Letters 214, 427-442.

Bridgwater, D., Collerson, K.D., Hurst, R.W., Jesseau, C.W., 1975. Field characters of the early Precambrian rocks from Saglek, coast of Labrador, Report of activities, part A. Geological Survey of Canada, Paper 75-1A, pp. 287–296.

Caro, G., Bourdon, B., Birck, J.L., Moorbath, S., 2003. $^{146}$Sm-$^{142}$Nd evidence from Isua metamorphosed sediments for early differentiation of the Earth's mantle. Nature 423, 428-432.

Cates, N.L., Mojzsis, S.J., 2007. Pre-3750 Ma supracrustal rocks from the Nuvvuagittuq supracrustal belt, northern Quebec. Earth and Planetary Science Letters 255, 9-21.

Collerson, K.D., Jesseau, C.W., Bridgwater, D., 1976. Crustal development of the Archaean Gneiss Complex: Eastern Labrador. In: Windley, B.F. (Ed.), The Early History of the Earth Based on the Proceeding of a NATO Advanced Study Institute Held at the University of Leicester 5–11 April, 1975. John Wiley & Sons, London, pp. 237–253.

Collerson, K.D., Bridgwater, D., 1979. Metamorphic development of early Archaean tonalitic and trondhjemitic gneisses: Saglek area, Labrador. In: Barker, F. (Ed.), Trondhjemites, Dacites, and Related Rock. Elsevier, Amsterdam.

Collerson, K.D., Campbell, L.M., Weaver, B.L., Palacz, Z.A., 1991. Evidence for Extreme Mantle Fractionation in Early Archean Ultramafic Rocks from Northern Labrador. Nature 349, 209-214.

Day, J.M.D., Pearson, D.G., Taylor, L.A., 2007. Highly siderophile element constraints on accretion and differentiation of the Earth-Moon system. Science 315, 217-219.

Day, J.M.D., Walker, R.J., 2015. Highly siderophile element depletion in the Moon. Earth and Planetary Science Letters 423, 114-124.

Debaille, V., O'Neill, C., Brandon, A.D., Haenecour, P., Yin, Q.Z., Mattielli, N., Treiman, A.H., 2013. Stagnant-lid tectonics in early Earth revealed by $^{142}$Nd variations in late Archean rocks. Earth and Planetary Science Letters 373, 83-92.

Fischer-Gödde, M., Becker, H., 2012. Osmium isotope and highly siderophile element constraints on ages and nature of meteoritic components in ancient lunar impact rocks. Geochimica et Cosmochimica Acta 77, 135-156.

Fischer-Gödde, M., Becker, H., Wombacher, F., 2011. Rhodium, gold and other highly siderophile elements in orogenic peridotites and peridotite xenoliths. Chemical Geology 280, 365-383.

Fonseca, R.O.C., Mallmann, G., O'Neill, H.S.C., Campbell, I.H., Laurenz, V., 2011. Solubility of Os and Ir in sulfide melt: Implications for Re/Os fractionation during mantle melting. Earth and Planetary Science Letters 311, 339-350.

Herrmann, W., Berry, R.F., 2002. MINSQ – a least squares spreadsheet method for calculating mineral proportions from whole rock major element analyses. Geochemistry: Exploration, Environment, Analysis 2, 361-368.

Komiya, T., Yamamoto, S., Aoki, S., Sawaki, Y., Ishikawa, A., Tashiro, T., Koshida, K., Shimojo, M., Aoki, K., Collerson, K.D., 2015. Geology of the Eoarchean, > 3.95 Ga, Nulliak supracrustal rocks in the Saglek Block, northern Labrador, Canada: The oldest geological evidence for plate tectonics. Tectonophysics 662, 40-66.

König, S., Munker, C., Schuth, S., Garbe-Schonberg, D., 2008. Mobility of tungsten in subduction zones. Earth and Planetary Science Letters 274, 82-92.

König, S., Munker, C., Hohl, S., Paulick, H., Barth, A.R., Lagos, M., Pfander, J., Buchl, A., 2011. The Earth's tungsten budget during mantle melting and crust formation. Geochimica et Cosmochimica Acta 75, 2119-2136.

Kruijer, T.S., Kleine, T., Fischer-Gödde, M., Sprung, P., 2015. Lunar tungsten isotopic evidence for the late veneer. Nature 520, 534-+.

Li, Y., Audétat, A., 2012. Partitioning of V, Mn, Co, Ni, Cu, Zn, As, Mo, Ag, Sn, Sb, W, Au, Pb, and Bi between sulfide phases and hydrous basanite melt at upper mantle conditions. Earth and Planetary Science Letters 355–356, 327-340.

McDonough, W.F., Sun, S.S., 1995. The Composition of the Earth. Chemical Geology 120, 223-253.

Mcgregor, V.R., 1973. Early Precambrian gneisses of Godthab district, West-Greenland. Philos T R Soc A 273, 343.

Nutman, A.P., Collerson, ö.D., 1991. Very early Archean crustal-accretion complexes preserved in the North Atlantic craton. Geology 19, 791-794.

O'Neil, J., Carlson, R.W., Francis, D., Stevenson, R.K., 2008. Neodymium-142 evidence for hadean mafic crust. Science 321, 1828-1831.

Puchtel, I.S., Touboul, M., Blichert-Toft, J., Walker, R.J., Brandon, A.D., Nicklas, R.W., Kulikov, V.S., Samsonov, A.V., 2016. Lithophile and siderophile element systematics of Earth's mantle at the Archean–Proterozoic boundary: Evidence from 2.4 Ga komatiites. Geochimica et Cosmochimica Acta 180, 227-255.

Rizo, H., Boyet, M., Blichert-Toft, J., Rosing, M., 2011. Combined Nd and Hf isotope evidence for deep-seated source of Isua lavas. Earth and Planetary Science Letters 312, 267-279.

Rizo, H., Boyet, M., Blichert-Toft, J., Rosing, M.T., 2013. Early mantle dynamics inferred from $^{142}$Nd variations in Archean rocks from southwest Greenland. Earth and Planetary Science Letters 377–378, 324-335.

Rizo, H., Walker, R.J., Carlson, R.W., Touboul, M., Horan, M.F., Puchtel, I.S., Boyet, M., Rosing, M.T., 2016. Early Earth Differentiation Investigated Through 142Nd, 182W, and Highly Siderophile Element Abundances in Samples From Isua, Greenland. Geochimica et Cosmochimica Acta 175, 319-336.

Roth, A.S.G., Bourdon, B., Mojzsis, S.J., Touboul, M., Sprung, P., Guitreau, M., Blichert-Toft, J., 2013. Inherited $^{142}$Nd anomalies in Eoarchean protoliths. Earth and Planetary Science Letters 361, 50-57.

Rudnick R. L. and Gao S. (2014) Composition of the continental crust. In Treatise on Geochemistry. Macmillan Publishers Limited, pp. 1–51.

Schiøtte, L., Compston, W., Bridgwater, D., 1989a. Ion Probe U-Th-Pb Zircon Dating of Polymetamorphic Orthogneisses from Northern Labrador, Canada. Canadian Jouranl of Earth Sciences 26, 1533-1556.

Schiøtte, L., Compston, W., Bridgwater, D., 1989b. U-Th-Pb Ages of Single Zircons in Archean Supracrustals from Nain Province, Labrador, Canada. Canadian Jouranl of Earth Sciences 26, 2636-2644.

Schiøtte, L., Noble, S., Bridgwater, D., 1990. U-Pb Mineral Ages from Northern Labrador - Possible Evidence for Interlayering of Early and Middle Archean Tectonic Slices. Geoscience Canada 17, 227-231.

Touboul, M., Liu, J., O'Neil, J., Puchtel, I.S., Walker, R.J., 2014. New insights into the Hadean mantle revealed by W-182 and highly siderophile element abundances of supracrustal rocks from the Nuvvuagittuq Greenstone Belt, Quebec, Canada. Chemical Geology 383, 63-75.

Touboul, M., Puchtel, I.S., Walker, R.J., 2012. W-182 Evidence for Long-Term Preservation of Early Mantle Differentiation Products. Science 335, 1065-1069.

Touboul, M., Puchtel, I.S., Walker, R.J., 2015. Tungsten isotopic evidence for disproportional late accretion to the Earth and Moon. Nature 520, 530-533.

Touboul, M., Walker, R.J., 2012. High precision tungsten isotope measurement by thermal ionization mass spectrometry. International Journal of Mass Spectrometry 309, 109-117.

Vockenhuber, C., Oberli, F., Bichler, M., Ahmad, I., Quitte, G., Meier, M., Halliday, A.N., Lee, D.C., Kutschera, W., Steier, P., Gehrke, R.J., Helmer, R.G., 2004. New half-life measurement of Hf-182: Improved chronometer for the early solar system. Physical Review Letters 93.

Walker, R.J., 2009. Highly siderophile elements in the Earth, Moon and Mars: Update and implications for planetary accretion and differentiation. Chem Erde-Geochem 69, 101-125.

Walker, R.J., Bermingham, K., Liu, J., Puchtel, I.S., Touboul, M., Worsham, E.A., 2015. In search of late-stage planetary building blocks. Chemical Geology 411, 125-142.

Wendt, J.I., Collerson, K.D., 1999. Early Archaean U/Pb fractionation and timing of late Archaean high-grade metamorphism in the Saglek-Hebron segment of the North Atlantic Craton. Precambrian Research 93, 281-297.

Willbold, M., Elliott, T., Moorbath, S., 2011. The tungsten isotopic composition of the Earth's mantle before the terminal bombardment. Nature 477, 195-198.

Willbold, M., Mojzsis, S.J., Chen, H.W., Elliott, T., 2015. Tungsten isotope composition of the Acasta Gneiss Complex. Earth and Planetary Science Letters 419, 168-177.

## Figure Captions

**Fig.1**. Geological sketch map of the Saglek-Hebron area of the North Atlantic Craton (inset map below), northern Labrador, Canada, modified after Schiøtte et al. (1986) and Wendt and Collerson (1999), with sample localities for this study marked.

**Fig. 2**. The concentrations and mass fractions of tungsten in constituent minerals and, where possible, grain-boundary assemblages for five Saglek samples (SB-13 – tonalite, SB-19 – amphibolite, KC87-104D – serpentinized dunite, KC91-32A– harzburgite, and KC87-114K– Websterite). $Bulk_m$: bulk composition measured; $Bulk_c$: bulk composition calculated by combining in situ mineral elemental concentrations with mineral modal abundance estimates calculated using the MINSQ program (Herrmann and Berry, 2002) from EPMA mineral and bulk rock XRF data (Table S1 & S2).

**Fig. 3**. Correlations between MgO (%) and W (ppm; A) or W/Th ratios (B) of the Saglek rocks. Also shown is the primitive mantle (PM; McDonough and Sun, 1995).

**Fig. 4**. W isotopic compositions ($\mu^{182}W$ - the deviation, in parts per million, of the $^{182}W/^{184}W$ ratio of a sample relative to the terrestrial reference standard) of the Labrador rocks. Each open symbol represents a single analysis, and each solid symbol represents the average if more than one analysis were performed. The grey field marks the 2σ SD uncertainty for long-term repeated analyses of the ESI standard (n = 31; **Fig. S5**), along with the results of a second standard: CPI and the Tristan da Cunha basalt 20171. Of note, sample KC87-114G (red square) has no resolvable difference ($\mu^{182}W = -2.6 \pm 4.6$; n=2; 2σ SD) from the terrestrial W isotopic standard.

**Fig. 5**. Correlations between W and Ba, U, Th, Ta, Zr and Hf contents for Saglek rocks. Primitive mantle (PM; McDonough and Sun, 1995) and MORB (König et al., 2008) data are shown for comparison. The enrichment or depletion of W relative to other lithophile elements is relative to modern mantle values.

**Fig. 6**. Correlation of $\mu^{182}W$ with W/Th ratio for the Saglek rock suite. Also shown is a model (see text for details) of metasomatic W addition to the assumed unaltered precursors of the Saglek ultramafic rocks, based on the premise that magmatic processes do not significantly fractionate the W/Th ratios; modeling marks represent increments of 10% W enrichment. Symbols are the same as **Fig. 5**.

**Fig. 7**. Average $\mu^{182}W$ data for the terrestrial Hadean to Proterozoic rocks with the magmatic emplacement ages marked. Also shown are the estimates of the pre-late accretionary terrestrial mantle taken from the pre-late accretionary lunar mantle (Touboul et al., 2015; Kruijer et al., 2015). Date sources: Guernsey gneiss from Willbold et al. (2011), Isua supracrustal rocks from Willbold et al. (2011) and Rizo et al. (2016), Komati and Kostomuksha komatiites from Touboul et al. (2012), Nuvvuagittuq supracrustal rocks from Touboul et al. (2014), Acasta Gneiss Complex from Willbold et al. (2015), and Vetreny komatiitic basalts and Vodla tonalites in the Fennoscandian Shield from Puchtel et al. (2016). For the Nuvvuagittuq supracrustal rocks, the emplacement age is controversial, ca. 3.75 Ga from Cates and Mojzsis (2007) or ca. 4.3 Ga from O'Neil et al. (2008).

Figure 1

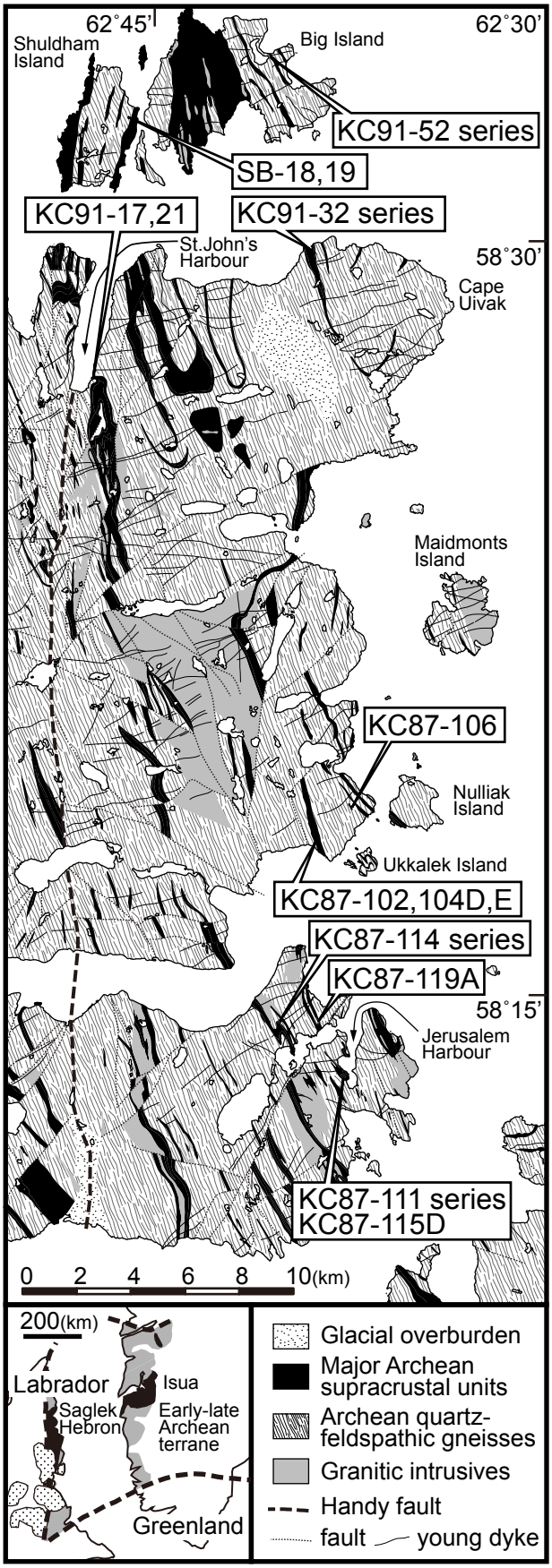
62°45'
62°30'
Shuldham Island
Big Island
KC91-52 series
SB-18,19
KC91-17,21
KC91-32 series
St.John's Harbour
58°30'
Cape Uivak
Maidmonts Island
KC87-106
Nulliak Island
Ukkalek Island
KC87-102,104D,E
KC87-114 series
KC87-119A
58°15'
Jerusalem Harbour
KC87-111 series
KC87-115D
0 2 4 6 8 10(km)
200(km)
Labrador
Isua
Saglek Hebron
Early-late Archean terrane
Greenland
Glacial overburden
Major Archean supracrustal units
Archean quartz-feldspathic gneisses
Granitic intrusives
Handy fault
fault
young dyke

Figure 2

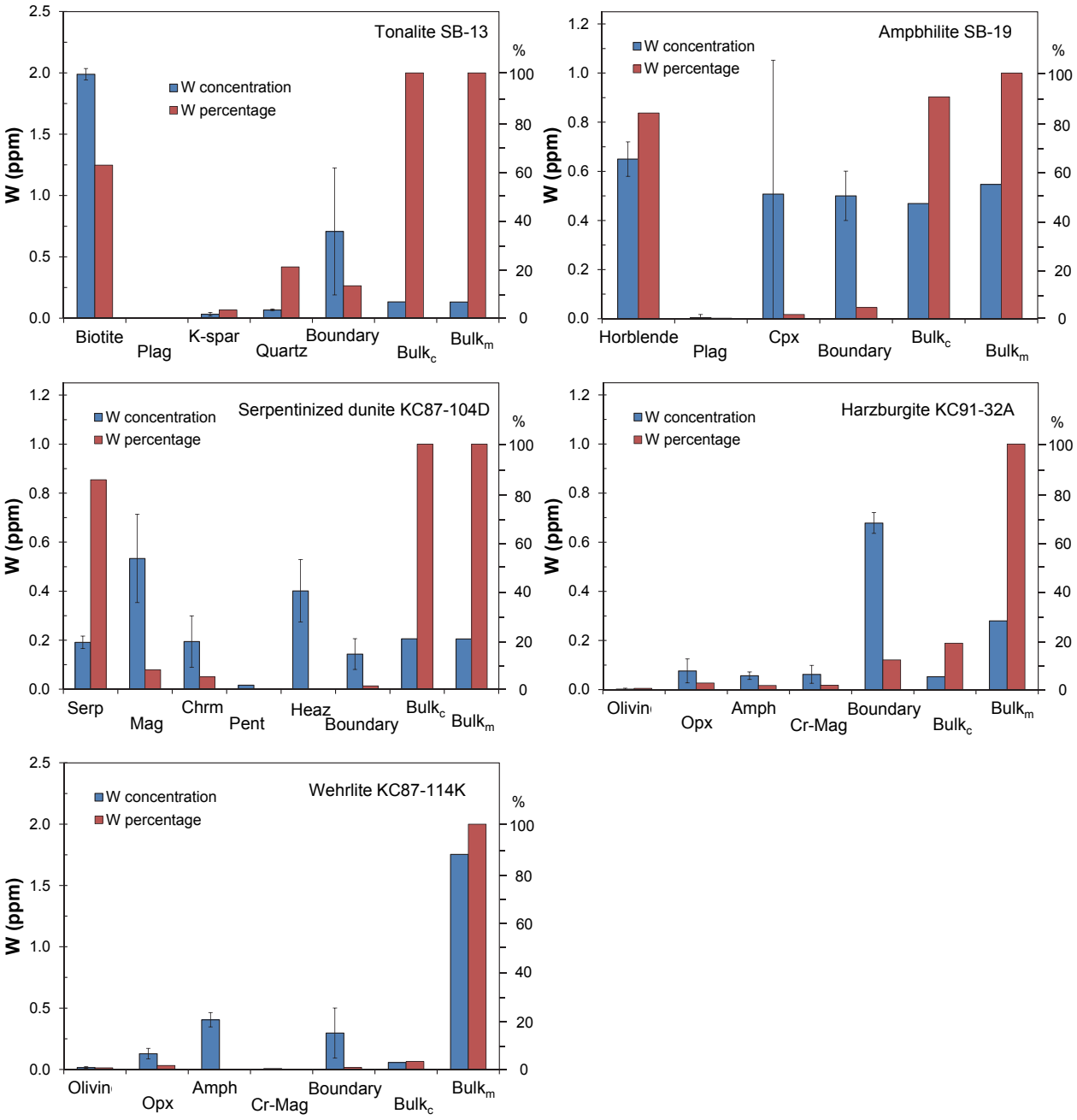
Tonalite SB-13
W concentration
W percentage
W (ppm)
%
Biotite
Plag
K-spar
Quartz
Boundary
Bulk$_c$
Bulk$_m$
Ampbhilite SB-19
Horblende
Plag
Cpx
Boundary
Bulk$_c$
Bulk$_m$
Serpentinized dunite KC87-104D
Serp
Mag
Chrm
Pent
Heaz
Boundary
Bulk$_c$
Bulk$_m$
Harzburgite KC91-32A
Olivin
Opx
Amph
Cr-Mag
Boundary
Bulk$_c$
Bulk$_m$
Wehrlite KC87-114K
Olivin
Opx
Amph
Cr-Mag
Boundary
Bulk$_c$
Bulk$_m$

Figure 3

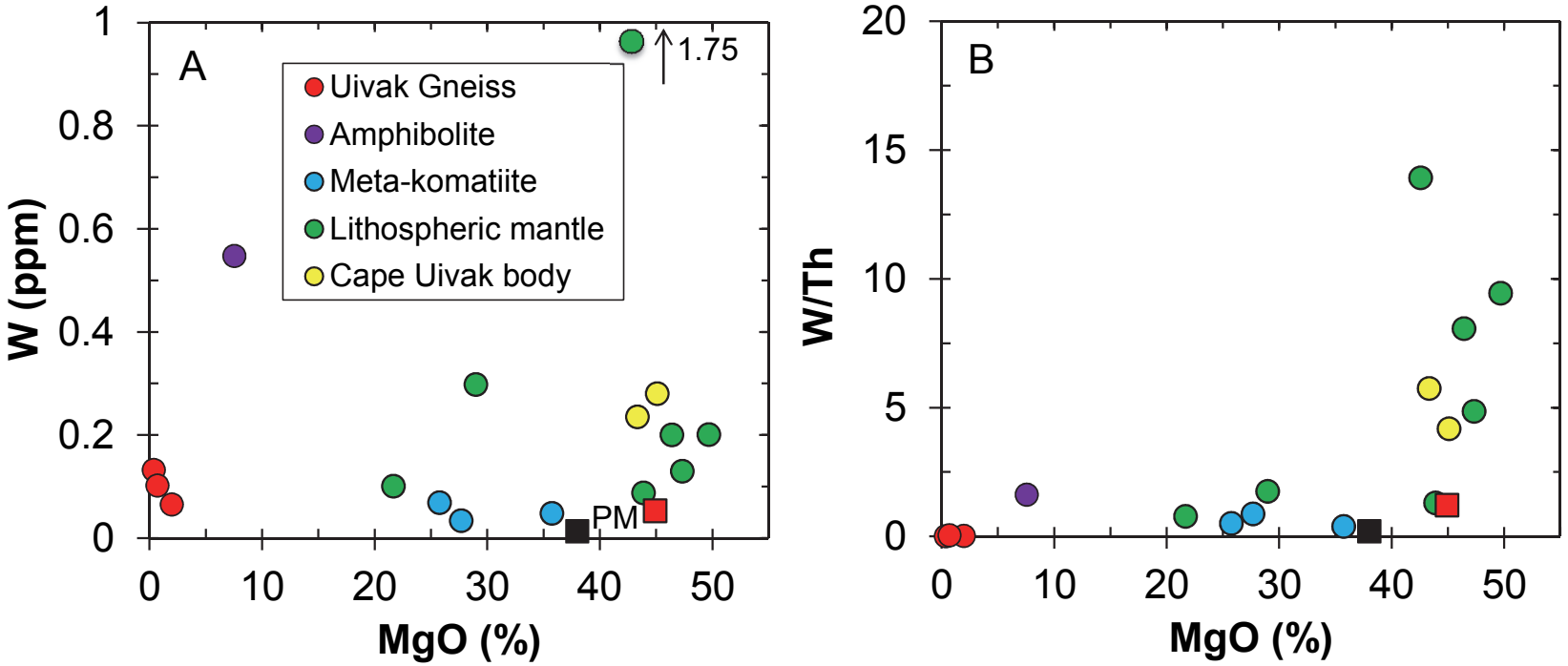
A
Uivak Gneiss
Amphibolite
Meta-komatiite
Lithospheric mantle
Cape Uivak body
1.75
PM
W (ppm)
MgO (%)
B
W/Th
MgO (%)

Figure 4

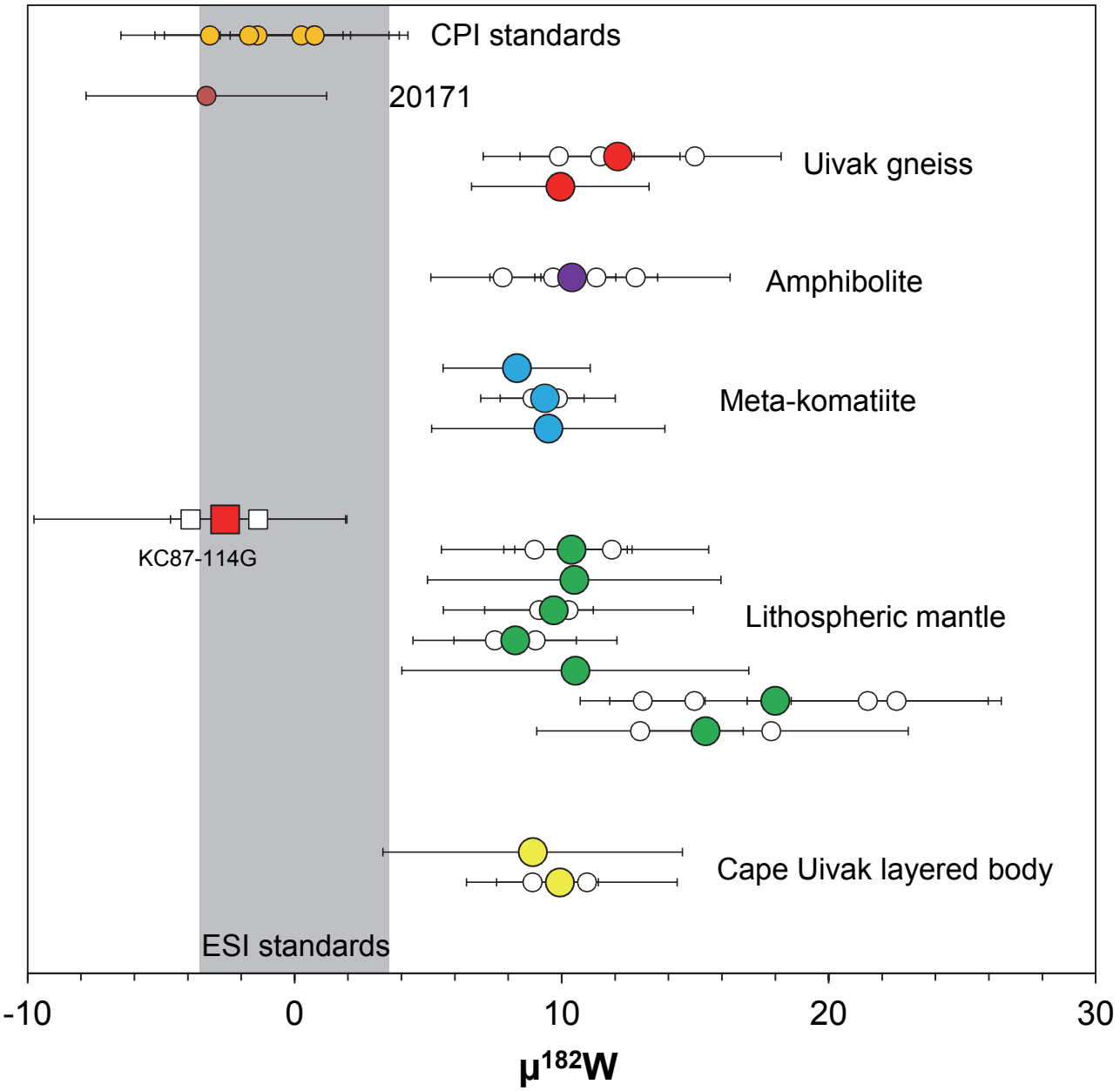
CPI standards
20171
Uivak gneiss
Amphibolite
Meta-komatiite
KC87-114G
Lithospheric mantle
Cape Uivak layered body
ESI standards
-10
0
10
20
30
μ182W

Figure 5

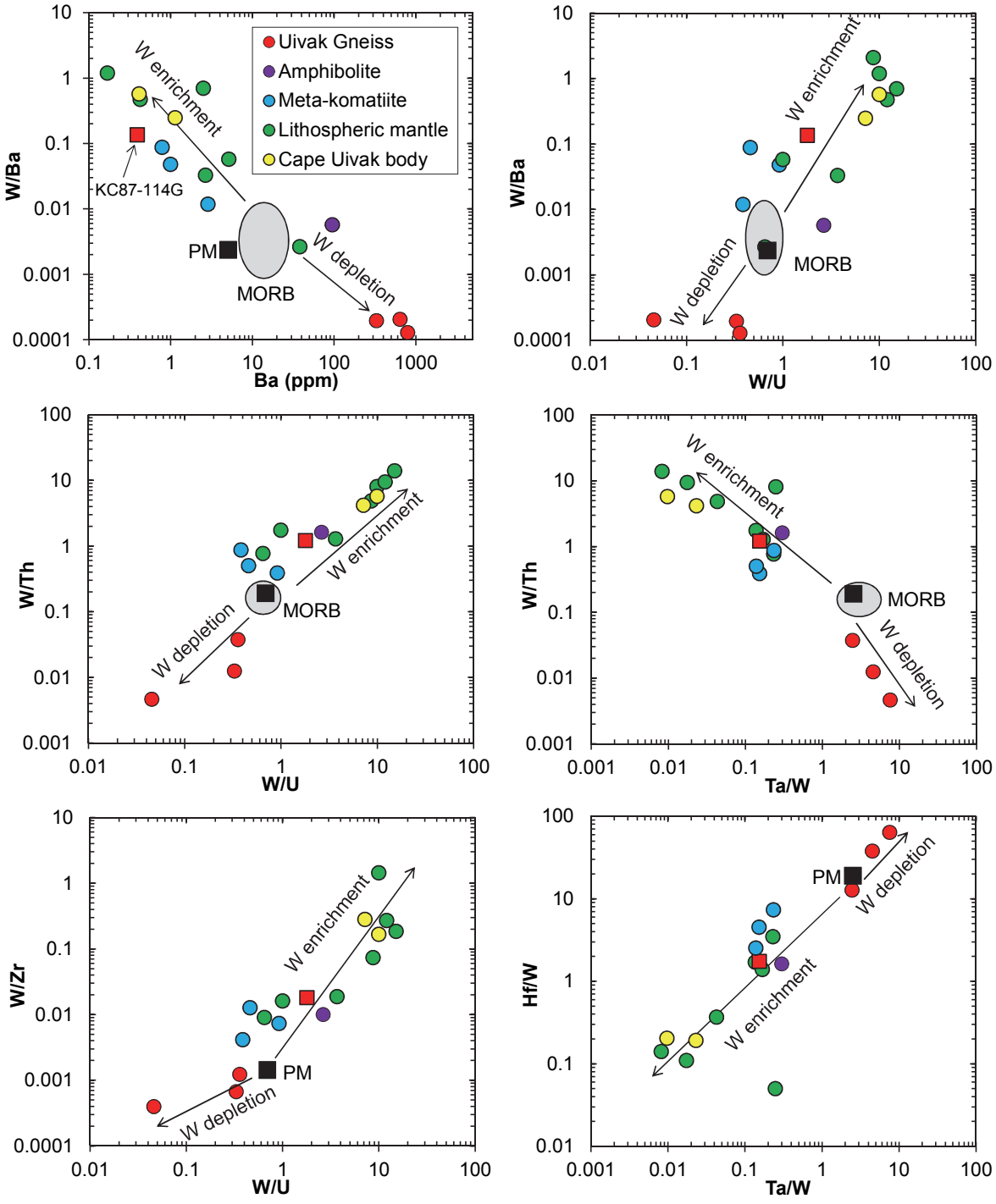
Uivak Gneiss
Amphibolite
Meta-komatiite
Lithospheric mantle
Cape Uivak body
W enrichment
W depletion
KC87-114G
PM
MORB
W/Ba
Ba (ppm)
W/U
W/Th
Ta/W
W/Zr
Hf/W

Figure 6

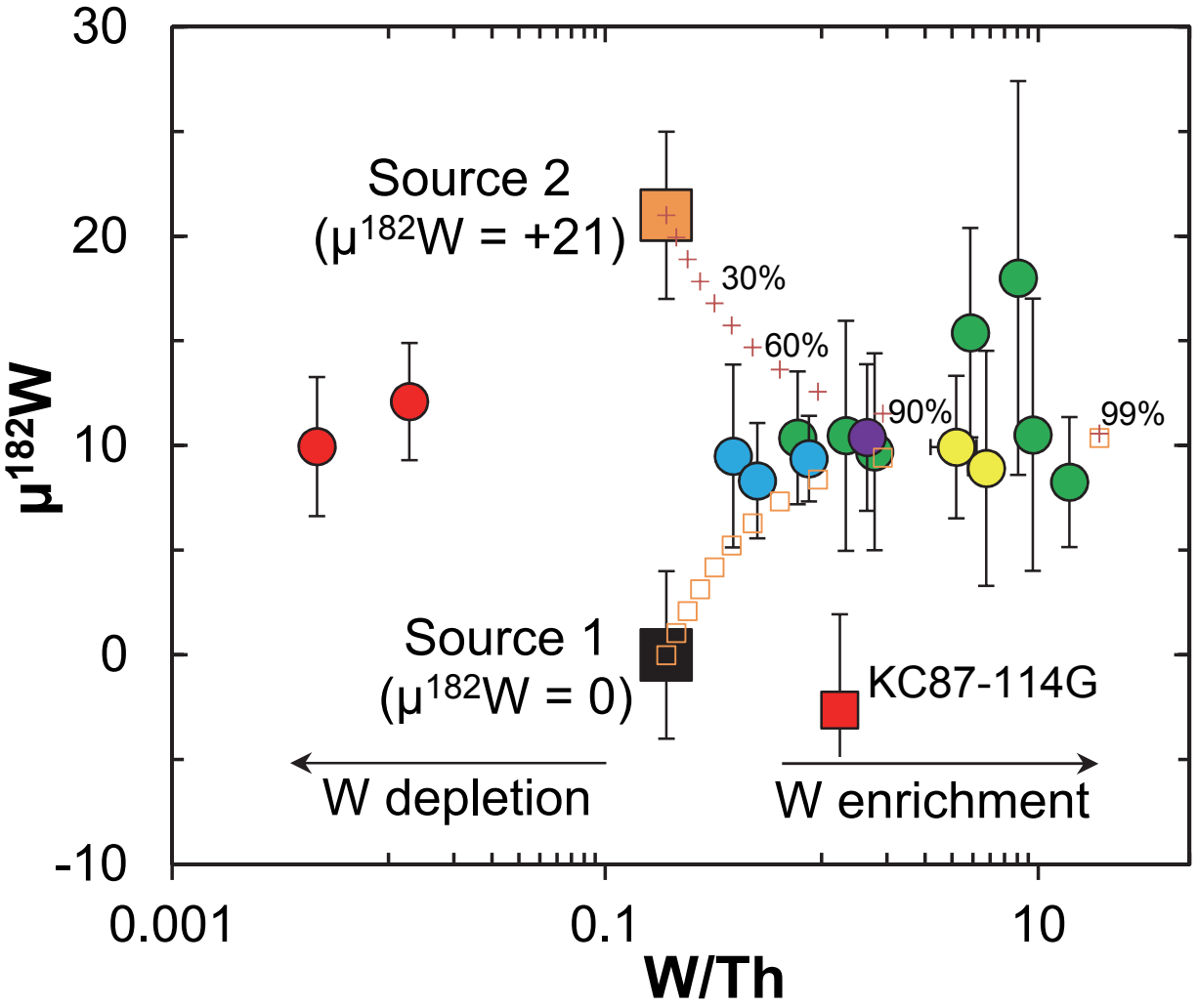
30
20
10
0
-10
μ182W
0.001
0.1
10
W/Th
Source 2
(μ182W = +21)
30%
60%
90%
99%
Source 1
(μ182W = 0)
KC87-114G
W depletion
W enrichment

Figure 7

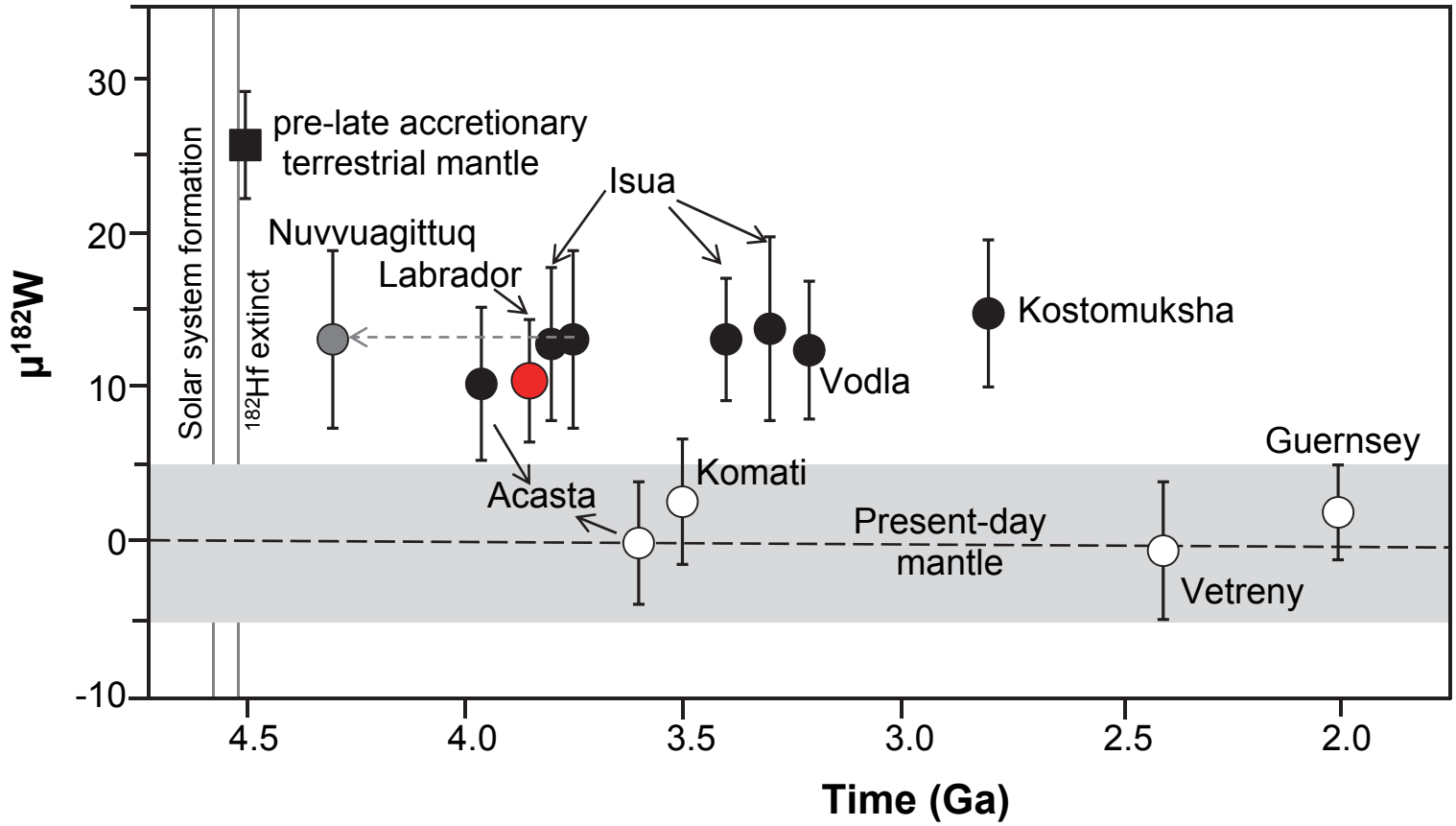
30
20
10
0
-10
μ182W
Solar system formation
182Hf extinct
pre-late accretionary
terrestrial mantle
Nuvvuagittuq
Labrador
Isua
Kostomuksha
Vodla
Guernsey
Komati
Acasta
Present-day
mantle
Vetreny
4.5
4.0
3.5
3.0
2.5
2.0
Time (Ga)

Table 1. Mineral W elemental composition determined by in situ Laser Ablation ICP-MS

| Samples/Phases | Modal abundance[a] | W ppm | 1σ | n[b] | W fraction[c] x100% |
|---|---|---|---|---|---|
| SB-13 | | | | | |
| Biotite | 4.1 | 1.989 | 0.046 | 2 | 0.624 |
| Plagioclase | 40.0 | 0 | 0 | 2 | 0 |
| K-spar | 13.4 | 0.033 | 0.013 | 2 | 0.034 |
| Quartz | 40.3 | 0.068 | 0.006 | 2 | 0.209 |
| Boundary | 2.5 | 0.707 | 0.517 | 4 | 0.133 |
| Bulk $rock_c$ | | 0.133 | | | 1 |
| Bulk $rock_m$ | | 0.132 | | | 1 |
| SB-19 | | | | | |
| Hornblende | 67.0 | 0.650 | 0.070 | 4 | 0.838 |
| Plagioclase | 26.2 | 0.005 | 0.012 | 4 | 0.002 |
| Clinopyroxene | 1.8 | 0.508 | 0.545 | 3 | 0.017 |
| Boundary | 5.0 | 0.500 | 0.101 | 2 | 0.046 |
| Bulk $rock_c$ | | 0.469 | | | 0.904 |
| Bulk $rock_m$ | | 0.547 | | | 1 |
| KC87-104d | | | | | |
| Serpentine | 89.9 | 0.192 | 0.025 | 2 | 0.855 |
| Magnetite | 3.0 | 0.534 | 0.180 | 4 | 0.079 |
| Chromite | 5.2 | 0.195 | 0.105 | 3 | 0.051 |
| Pentlandite | 0.1 | 0.017 | | 1 | 0.000 |
| Heazelwoodite | 0.1 | 0.401 | 0.127 | 3 | 0.002 |
| Boundary | 2 | 0.143 | 0.063 | 3 | 0.014 |
| Bulk $rock_c$ | | 0.206 | | | 1 |
| Bulk $rock_m$ | | 0.205 | | | 1 |
| KC91-32A | | | | | |
| Olivine | 67.7 | 0.002 | 0.004 | 3 | 0.006 |
| Orthopyroxene | 9.4 | 0.076 | 0.049 | 4 | 0.027 |
| Amphibole | 8.1 | 0.057 | 0.015 | 2 | 0.017 |
| Cr-Magnetite | 7.8 | 0.062 | 0.037 | 7 | 0.018 |
| Boundary | 5.0 | 0.679 | 0.042 | 2 | 0.121 |
| Bulk $rock_c$ | | 0.053 | | | 0.189 |
| Bulk $rock_m$ | | 0.280 | | | 1 |
| KC87-114K | | | | | |
| Olivine | 72.5 | 0.016 | 0.007 | 2 | 0.007 |
| Pargasite | 21.2 | 0.129 | 0.042 | 2 | 0.016 |
| Cr Magnetite | 0.3 | 0.405 | 0.058 | 3 | 0.001 |
| Spinel | 1.0 | 0.007 | 0.000 | 4 | 0.000 |
| Boundary | 5.0 | 0.297 | 0.203 | 7 | 0.008 |
| Bulk $rock_c$ | | 0.057 | | | 0.032 |
| Bulk $rock_m$ | | 1.754 | | | 1 |

Note: Bulk $rock_c$ and Bulk $rock_m$ represent the bulk rock composition calculated and measured, respectively.

a. Mineral modal abunance estimates are calculated using the MINSQ program (Herrmann and Berry, 2002) from EPMA mineral and bulk rock XRF data.

b. 'n' represents the number of mineral grains with one analysis per grain.

c. Mineral/calculated bulk W fraction in the measured bulk rock.

Table 2. Tungsten concentration and isotopic composition of Archean felsic, mafic and ultramafic rocks from Labrador, Canada, and of the modern basalt 20171 and CPI standard

| Sample | Lithology | $Al_2O_3$ | MgO | LOI | W | Th | W/Th | W isotopic composition | | |
|---|---|---|---|---|---|---|---|---|---|---|
| | | % | % | % | ppb | ppb | | $\mu^{182}W$ | 2σ | n |
| *Uivak gneiss* | | | | | | | | | | |
| KC91-17 | Tonalitic gneiss | 17.64 | 1.97 | 0.68 | 65 | 5220 | 0.012 | 12.1 | 3.2 | 3 |
| SB-13 | Tonalitic gneiss | 12.85 | 0.37 | 0.50 | 132 | 28335 | 0.0047 | 10.0 | 3.3 | 1 |
| SB-18 | Tonalitic gneiss | 15.94 | 0.70 | 0.37 | 102 | 2722 | 0.037 | | | |
| average | | | | | | | | 11.0 | 3.3 | 3 |
| SB-19 | Amphibolite | 15.48 | 7.55 | 0.41 | 547 | 338 | 1.62 | 10.4 | 3.5 | 4 |
| *Meta-komatiite suite* | | | | | | | | | | |
| KC87-111E | Pyroxene hornblendite | 5.65 | 27.7 | 0.59 | 69 | 137 | 0.51 | 8.3 | 2.8 | 1 |
| KC87-111F | Olivine-pyroxene hornblendite | 8.55 | 27.1 | 0.97 | 35 | | | | | |
| KC87-111G | Olivine-pyroxene hornblendite | 4.34 | 35.7 | 3.53 | 48 | 123 | 0.39 | 9.5 | 4.4 | 1 |
| KC87-111I | Olivine hornblendite | 9.63 | 30.2 | 7.77 | 47 | | | | | |
| KC87-111K | Olivine hornblendite | 6.66 | 25.8 | 1.20 | 34 | 39 | 0.88 | 9.4 | 2.0 | 2 |
| average | | | | | | | | 9.1 | 3.4 | 3 |
| *Lithospheric mantle Suite* | | | | | | | | | | |
| KC87-104D | Dunite | 0.02 | 46.4 | 16.0 | 205 | 25 | 8.29 | 18.0 | 4.7 | 4 |
| KC87-104E | Meta-harzburgite | 0.14 | 45.5 | 8.23 | 697 | | | | | |
| KC91-21A | Dunite | 0.95 | 43.9 | 1.88 | 70 | | | | | |
| KC91-21B | Dunite | 0.53 | 46.8 | 0.12 | 144 | | | | | |
| KC91-52A | Dunite | 0.64 | 42.0 | 11.1 | - | | | | | |
| KC91-52B | Dunite | 0.54 | 47.3 | 3.30 | 131 | 27 | 4.88 | 15.4 | 5.0 | 2 |
| KC91-52C | Hornblendite | 5.39 | 29.0 | 5.40 | 297 | 170 | 1.75 | 9.7 | 4.7 | 2 |
| KC91-52D | Dunite | 0.35 | 49.7 | 2.09 | 201 | 21 | 9.45 | 10.5 | 6.5 | 1 |
| KC87-114G | Meta-harzburgite | 1.36 | 44.9 | 10.2 | 53 | 44 | 1.20 | -2.6 | 4.6 | 2 |
| KC87-114I | Meta-lherzolite | 1.90 | 43.9 | 5.96 | 88 | 68 | 1.30 | 10.5 | 5.5 | 1 |
| KC87-114K | Meta-olivine websterite | 2.79 | 42.6 | 1.41 | 1754 | 126 | 13.9 | 8.3 | 3.1 | 2 |
| KC87-119A | Meta-olivine websterite | 4.06 | 35.8 | 1.62 | - | | | | | |
| KC87-102 | Olivine hornblendite | 4.49 | 36.2 | 9.27 | 105 | | | | | |
| KC87-106A | Meta-pyroxenite | 5.39 | 21.7 | 1.35 | 102 | 131 | 0.778 | 10.4 | 3.2 | 3 |
| average | | | | | | | | 11.8 | 7.0 | 7 |
| *Cape Uivak layered body* | | | | | | | | | | |
| KC91-32A | Amphibole harzburgite | 1.28 | 45.1 | 2.45 | 287 | 67 | 4.28 | 9.9 | 3.4 | 2 |
| KC91-32B | Amphibole harzburgite | 1.15 | 43.4 | 3.07 | 248 | | | | | |
| KC91-32C-1 | Olivine hornblendite | 4.07 | 26.2 | 3.02 | 200 | | | | | |
| KC91-32C-3 | Olivine hornblendite | 4.86 | 27.4 | 2.65 | 170 | | | | | |
| KC91-32D | Amphibole harzburgite | 1.47 | 45.6 | 3.86 | 220 | | | | | |
| KC91-32E | Amphibole harzburgite | 0.79 | 43.3 | 6.65 | 235 | 41 | 5.74 | 8.9 | 5.6 | 1 |
| KC91-32F | Amphibole harzburgite | 1.36 | 44.8 | 3.21 | 196 | | | | | |
| average | | | | | 222 | | | 9.4 | 4.8 | 2 |
| average of all the ultramafic rocks above | | | | | | | | 10.7 | 2.9 | 12 |
| 20171 | Tristan da Cunha basalt | | | | 1143 | | | -3.3 | 4.5 | 1 |
| CPI | Standard | | | | | | | -0.8 | 3.2 | 6 |

*Electronic Supplement for*

# Widespread tungsten isotope anomalies and W mobility in crustal and mantle rocks of the Eoarchean Saglek Block, northern Labrador, Canada: Implications for early Earth processes and W recycling

Jingao Liu[1,*], Mathieu Touboul[2,**], Akira Ishikawa[3,4], Richard J. Walker[2], D. Graham Pearson[1]

[1] Department of Earth and Atmospheric Sciences, University of Alberta, 1-26 Earth Sciences Building, Edmonton, Alberta T6G 2E3 Canada

[2]Department of Geology, University of Maryland, College Park, Maryland, 20742 USA

[3]Department of Earth Science and Astronomy, University of Tokyo, 3-8-1 Komaba, Meguro, Tokyo 153-8902, Japan

[4]Research and Development Center for Submarine Resources, Japan Agency for Marine Earth Science and Technology (JAMSTEC), Yokosuka 236-0016, Japan

Contents:

## Appendix 1: analytical methods

### 1.1. Mineral major element analyses by Electron Probe Microanalyzer

Mineral major element compositions were measured using a JEOL 8900 Electron Probe Microanalyzer (EPMA) at the University of Alberta. The analyses were performed using wavelength dispersive spectroscopy with a 15 kV accelerating voltage, a 20 nA cup current, and a 10 μm diameter beam. A variety of natural minerals were used as standards (see the standard list in http://www.eas.ualberta.ca/eml/?page=standards), and raw x-ray intensities were corrected using a ZAF algorithm. Average values of 2 to 4 points are reported for each mineral. The data are shown in Table S1.

### 1.2. In situ W analyses by in situ LA-ICP-MS

Mineral tungsten data were obtained on polished thick sections using *in situ* laser ablation coupled with inductively coupled plasma-mass spectrometry (LA-ICP-MS) at the University of Alberta. The laser ablation used was a Resonetics M-50 193nm excimer laser system connected, via Nylon tubing, to a high resolution sector-field ICP-MS Thermo Element XR. The mass spectrometer was operated in low mass resolution mode (M/ΔM=ca. 300). Minerals were ablated using 75 μm craters and a 5 Hz repetition with the laser energy at the target (fluence) regulated at ~4 J/cm$^2$. An analysis comprised 30 s of background gas collection followed by 60 s of ablation. Ablated aerosols were entrained in a He cell gas flow (600 mL/min) and subsequently mixed with $N_2$ (2 mL/min) and Ar (0.8 mL/min) prior to entering the ICP-MS torch. The ICP-MS was operated at 1300W and a torch depth of 3.6 mm. Argon and helium gas flow, torch position and focusing potentials were optimized in order to achieve optimal signals on Co, La and Th and low oxide production rates (ThO/Th<0.5%). Isotopes monitored (averages for more than one isotope) were: $^{43}$Ca, $^{47}$Ti, $^{49}$Ti, $^{57}$Fe, $^{90}$Zr, $^{93}$Nb, $^{95}$Mo, $^{98}$Mo, $^{120}$Sn, $^{121}$Sb, $^{135}$Ba, $^{137}$Ba, $^{140}$Ce, $^{178}$Hf, $^{181}$Ta, $^{182}$W, $^{184}$W, $^{208}$Pb and $^{238}$U. Calibration was performed using NIST SRM 612 in conjunction with isotope $^{43}$Ca as the internal standard or using MSS-1 with $^{57}$Fe as the internal standard. All data were reduced offline using Iolite v3 (https://iolite-software.com/). The W results of the secondary standards (e.g., NIST614) agree with the reference values within relative uncertainties of typical 5–10% or better at the 95% confidence level. For the sample phases, the uncertainties of W data negatively correlate with the W concentrations ranging from ~4% for phases with W >0.4 ppm to higher values for phases with lower concentrations, typically less than 30%, but as high as 100% for phases like olivine and plagioclase with ppb to sub-ppb W concentrations. The reported data are based on the usage of internal standard (either $^{43}$Ca or $^{57}$Fe, or both with averages taken as shown in Table 1).

### 1.3. Whole-rock major element analyses

Whole-rock major and minor element compositions and loss-on-ignition values were determined by X-ray fluorescence (XRF) on fused glass disks made from powders (see Boyd and Mertzman (1987) for detailed protocols) at Franklin and Marshall College, United States or at the University of Tokyo. Analytical precision and accuracy was typically better than 1% for major elements of concentrations greater than 0.5% and better than 5% for the remaining major and minor elements, as determined from data for international reference rocks in this lab (Boyd and Mertzman, 1987; the data of BHVO-2 can be found in http://www.fandm.edu/earth-environment/laboratory-facilities/instrument-use-and-instructions/precision-accuracy). These data, along with previous published data for some samples, are reported in Table S2.

### 1.4. Whole-rock trace element analyses

Whole-rock trace element analyses followed the protocol of Ottley et al. (2003). Powder aliquots of ~50 mg for both samples and reference materials (including BHVO-2, BIR-1, BCR-1, AGV-2, and DST-1) were digested in 7 ml pre-cleaned, screw-cap Teflon beakers using a mixture of concentrated HF (2 ml) and $HNO_3$ (0.5 ml) for at least 48 hours at 150°C, as well as the preparation of several blanks in the same course. After digestion, the HF/$HNO_3$ mixture was evaporated to near dryness and repeatedly treated by $HNO_3$ to drive off the initial HF/$HNO_3$ mixture. The samples were finally dissolved in 2.5 ml of concentrated $HNO_3$ followed by adding 2.5ml of Milli-Q $H_2O$ overnight at 100°C. After cooling, the samples were further diluted to exactly 50ml using water, to make a solution in approximately 3% $HNO_3$ ready for ICP-MS. The samples were further diluted by 3% $HNO_3$ along with doping In as an internal standard to correct instrumental drifting, and measured using an Thermo Fisher Element XR ICP-MS at the University of Alberta. Reference material BHVO-2 was taken as the standard for data reduction and other reference materials were taken as unknowns. Data were reduced offline using Iolite v3 (https://iolite-software.com/), and reported in Table S2, along with previously published data for some samples, while the data for the reference materials are shown in Table S3.

### 1.5.Tungsten concentrations

Whole-rock tungsten concentrations cannot be precisely determined along with other trace elements as discussed in section 1.4 primarily due to relatively low concentrations and potential higher procedural blanks. Here W concentrations were measured by isotope dilution using an $^{182}W$-enriched spike at the University of Maryland or the University of Alberta. Powder aliquots of 100-700 mg were digested in 15 or 7 mL screw-cap Teflon vials using a mixture of concentrated HF and $HNO_3$ acids (4:1) at 180ºC for at least 3 days. After digestion, the solutions were dried down, and the residues were treated twice using concentrated $HNO_3$ and traces of

30% $H_2O_2$ at 120ºC. After evaporation to dryness, residues were converted into chloride by addition of 6N HCl, followed by a second evaporation to dryness. Samples were then dissolved in 6N HCl-0.01N HF overnight at 120ºC, whereupon complete dissolution (i.e., clear solution) was normally achieved. Finally, solutions were dried down again and residues were then re-dissolved in 2ml of a 0.5N HCl - 0.5N HF mixture, and W was then separated and purified for ICP-MS measurements using anion exchange chromatography established previously by Kleine et al. (2004). The isotopic compositions of the sample-spike mixtures were measured using the Nu Plasma ICP-MS at the University of Maryland or the Thermo-Fisher Element XR ICP-MS at the University of Alberta. Procedural W blanks during the analytical campaign were averaged 0.30 ± 0.08 ng (n=4), corresponding to contributions of generally less than 2% of the total W present in the samples.

### 1.6. High-precision tungsten isotope compositions

The chemical and instrumental procedures followed the protocol of Touboul and Walker (2012) and were conducted at the University of Maryland or University of Alberta. Based on W concentrations determined by isotope dilution, ~3 to 32 g of sample powder were processed to yield ~2 μg of W necessary for analysis on mass spectrometry. Powder aliquots were dissolved in 60 or 180 mL Teflon vials using a mixture of concentrated HF and $HNO_3$ acids (5:1) more than five days at 150ºC. After evaporation of the HF-$HNO_3$ solutions, residues were treated twice using concentrated $HNO_3$ in combination with traces of 30% $H_2O_2$, over ~24 hours at 120ºC, followed by evaporation to dryness. Residues were then converted into the chloride form by repeated dissolutions using 6N HCl and subsequent evaporations to dryness. The samples were finally dissolved in 10 to 40 mL 1N HCl-0.1N HF. After centrifugation, W in the supernatant was separated and purified using a four-step cation/anion exchange chromatography protocol, allowing W separation from large samples. Tungsten recovery using this procedure was better than 90% for all samples analyzed here.

Tungsten isotope measurements were conducted by N-TIMS, as described in detail in Touboul and Walker (2012), using the Thermo-Fisher Triton Plus at the University of Alberta. This analytical technique permitted achievement of ± 4 ppm external precision (2σ SD) on the $^{182}W/^{184}W$ ratio (see Fig. S5). Procedural blanks averaged ~1.8 ng at the University of Maryland and ~5 ng at the University of Alberta, both contributing less than 0.3% of total W present in the sample. Blank corrections on measured W isotope composition were negligible and therefore not implemented. The results of the modern La Palma LP15 digested and measured in the University of Maryland in a prior study of the group (Touboul et al., 2012) showed identical W isotopic compositions to the modern mantle ($\mu^{182}W$ = 0.2±2.9; 2σ; n=3). The analysis of the Tristan da Cunha basalt 20171 digested and measured in the University of Alberta in this study yielded a $\mu^{182}W$ of -3.3 ± 4.5 (2σ).

**References cited:**

Boyd, F.R., Mertzman, S.A., 1987. Composition of structure of the Kaapvaal lithosphere, southern Africa. In: Magmatic Processes - Physicochemical Principles, B.O. Mysen, Ed., The Geochemical Society, Special Publication 1.

Herrmann, W., Berry, R.F., 2002. MINSQ – a least squares spreadsheet method for calculating mineral proportions from whole rock major element analyses. Geochemistry: Exploration, Environment, Analysis 2, 361-368.

Ishikawa, A., Senda, R., Suzuki, K., Dale, C.W. and Meisel, T., 2014. Re-evaluating digestion methods for highly siderophile element and $^{187}Os$ isotope analysis: Evidence from geological reference materials. Chemical Geology 384, 27-46.

Kleine, T., Mezger, K., Münker, C., Palme, H., Bischoff, A., 2004. 182Hf-182W isotope systematics of chondrites, eucrites, and martian meteorites: Chronology of core formation and early mantle differentiation in Vesta and Mars1. Geochimica et Cosmochimica Acta 68, 2935-2946.

McDonough, W.F., Sun, S.S., 1995. The Composition of the Earth. Chemical Geology 120, 223-253.

Ottley, C.J., Pearson, D.G., Irvine, G.J., 2003. A routine method for the dissolution of geological samples for the analysis of REE and trace elements via ICP-MS. Plasma Source Mass Spectrometry: Applications and Emerging Technologies, 221-230.

Touboul, M., Walker, R.J., 2012. High precision tungsten isotope measurement by thermal ionization mass spectrometry. International Journal of Mass Spectrometry 309, 109-117.

## Appendix 2: Supplementary figures

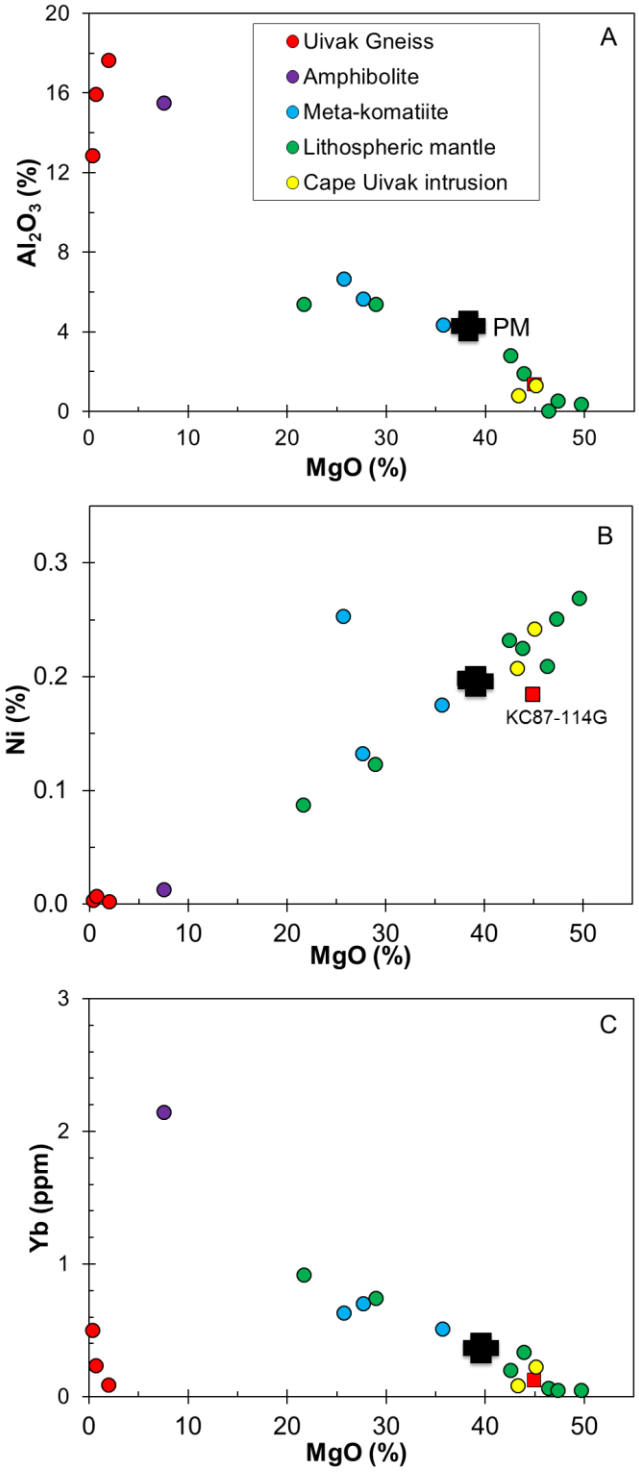


**Fig. S1**. Correlations between MgO (%) and $Al_2O_3$ (%; A) or Ni (%; B) or Yb (ppm; C)contents of the rocks from northern Labrador, Canada. Also shown is the primitive mantle (PM) (McDonough and Sun, 1995).

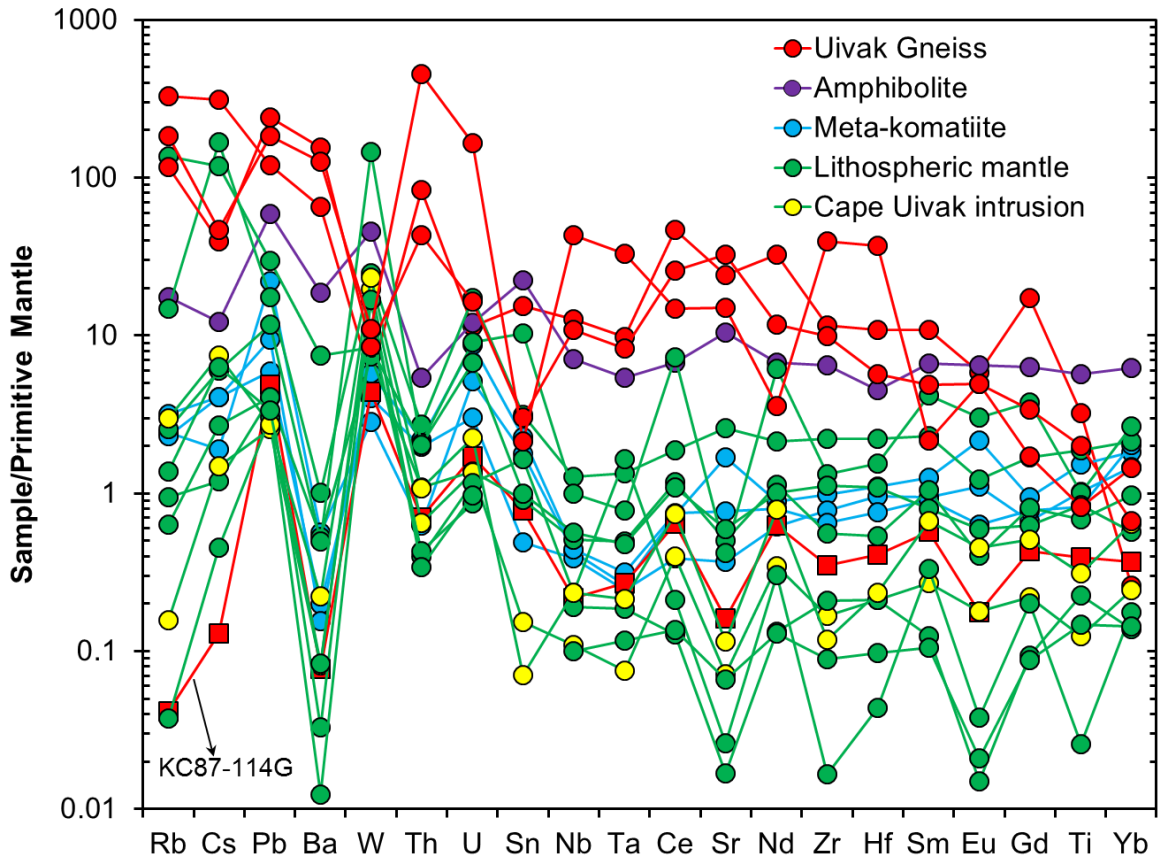


**Fig. S2**. Primitive mantle-normalized trace element spider diagram for the rocks from northern Labrador, Canada. Primitive mantle data are from McDonough and Sun (1995).

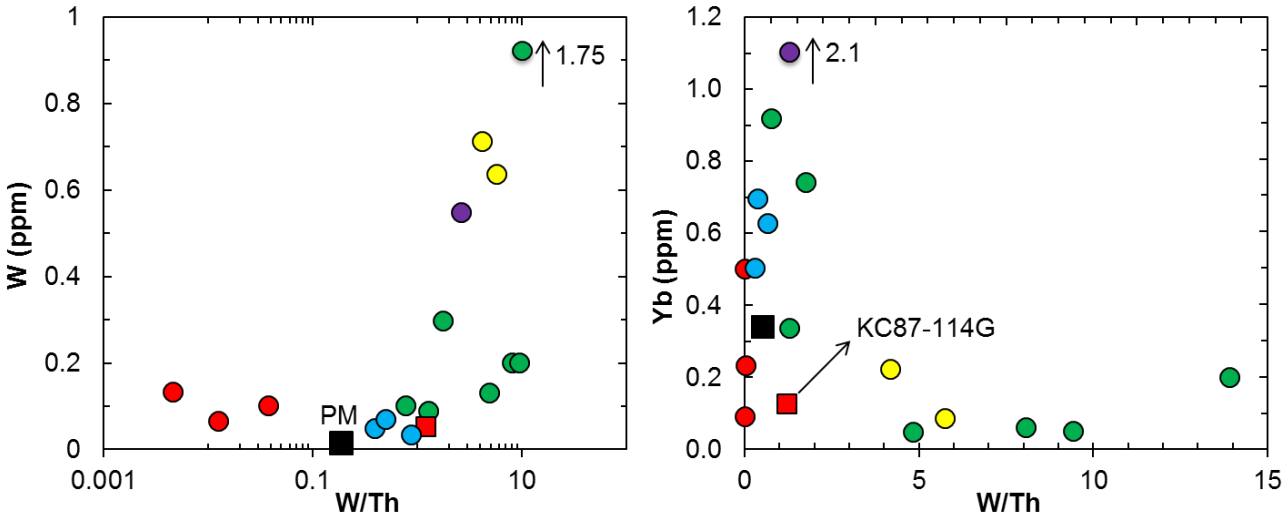


**Fig. S3**. Correlations between W/Th ratios versus W or Yb content of the rocks from northern Labrador, Canada. Symbols are the same as in **Fig. S1**.

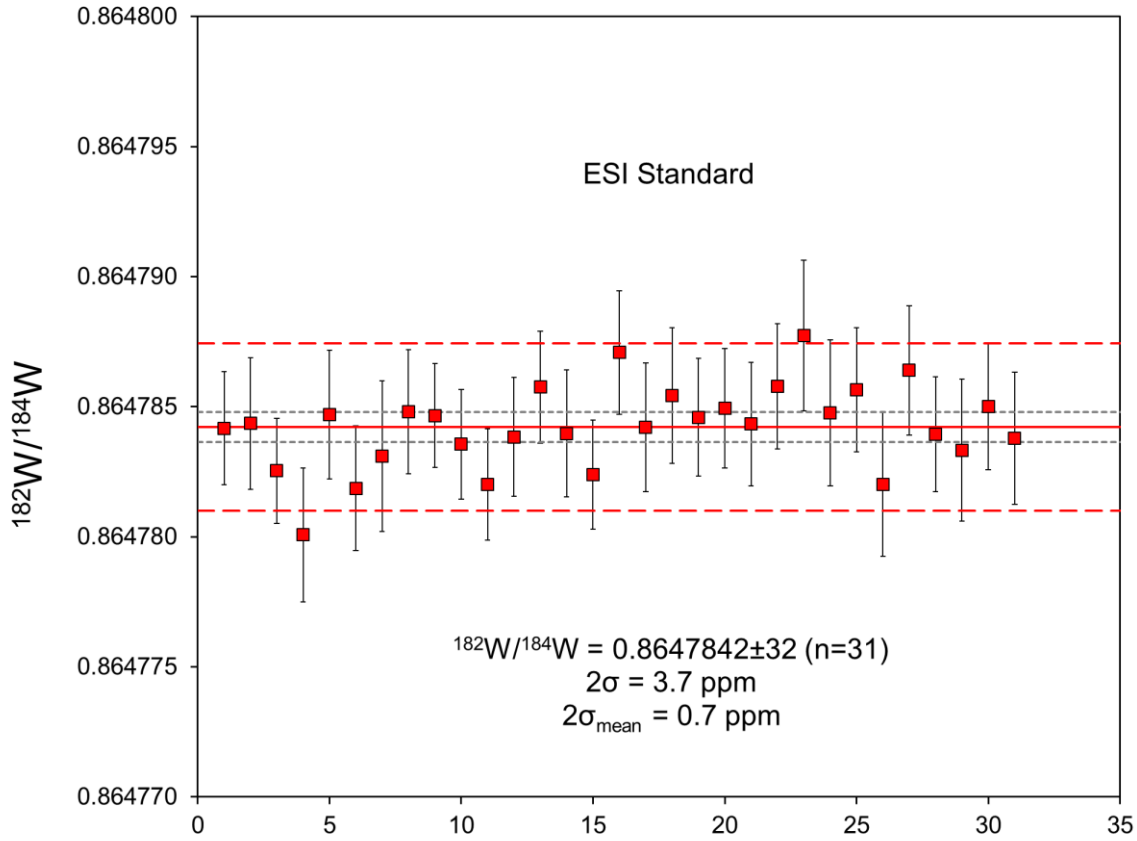


**Fig. S4**. Long-term $^{182}W/^{184}W$ ratio of ESI standard measured on loads of ~1µg W on Re filaments at the University of Alberta during the analytical course of the samples (December 2013 to July 2014).